DISCLAIMER

This report was prepared as an account of work sponsored by an agency of the United States Government. Neither the United States Government nor any agency thereof, nor Battelle Memorial Institute, nor any of their employees, makes any warranty, express or implied, or assumes any legal liability or responsibility for the accuracy, completeness, or usefulness of any information, apparatus, product, or process disclosed, or represents that its use would not infringe privately owned rights. Reference herein to any specific commercial product, process, or service by trade name, trademark, manufacturer, or otherwise does not necessarily constitute or imply its endorsement, recommendation, or favoring by the United States Government or any agency thereof, or Battelle Memorial Institute. The views and opinions of authors expressed herein do not necessarily state or reflect those of the United States Government or any agency thereof.

PACIFIC NORTHWEST NATIONAL LABORATORY
operated by
BATTELLE
for the
UNITED STATES DEPARTMENT OF ENERGY
under Contract DE-AC06-76RLO 1830

Printed in the United States of America

Available to DOE and DOE contractors from the Office of Scientific and Technical Information, P.O. Box 62, Oak Ridge, TN 37831; prices available from (615) 576-8401.

Available to the public from the National Technical Information Service, U.S. Department of Commerce, 5285 Port Royal Rd., Springfield, VA 22161


This document was printed on recycled paper.
(9/97)

PNNL-11706
UC-2030

Pacific Northwest
National Laboratory

Operated by Battelle for the
U.S. Department of Energy

Waste Behavior During Horizontal Extrusion: Effect of Waste Strength for Bentonite and Kaolin/Ludox Simulants and Strength Estimates for Wastes from Hanford Waste Tanks 241-SY-103, AW-101, AN-103, and S-102

P. A. Gauglitz
J. T. Aikin

October 1997

RECEIVED
NOV 10 1997
OSTI

Prepared for the U.S. Department of Energy
under Contract DE-AC06-76RLO 1830

PNNL-11706
UC-2030

Waste Behavior During Horizontal Extrusion: Effect of Waste Strength for Bentonite and Kaolin/Ludox Simulants and Strength Estimates for Wastes from Hanford Waste Tanks 241-SY-103, AW-101, AN-103, and S-102

P. A. Gauglitz
J. T. Aikin

October 1997

Prepared for
the U.S. Department of Energy
under Contract DE-AC06-76RLO 1830

Pacific Northwest National Laboratory
Richland, Washington 99352

Executive Summary

The Hanford Site has 149 single-shell tanks (SSTs) and 28 double-shell tanks (DSTs) containing radioactive wastes that are complex mixes of radioactive and chemical products. Some of these wastes are known to generate mixtures of flammable gases, including hydrogen, nitrous oxide, and ammonia. Nineteen of these SSTs and six of the DSTs have been placed on the Flammable Gas Watch List because they are known or suspected, in all but one case, to retain these flammable gases. Because these gases are flammable, their retention and episodic release pose a number of safety concerns. Understanding the physical mechanisms and waste properties that contribute to the retention and release of these gases will help to resolve the Flammable Gas Safety Issue.

The strength of the waste plays a central role in the mechanisms of both bubble retention and bubble release. While recent in-situ measurements from the ball rheometer have provided results for five of the DSTs, waste strength measurements are typically not available for any of the SSTs or for the DSTs that have not been characterized with the ball rheometer.

The overall purpose of this study is to develop a method to obtain strength estimates for actual wastes from observations of the wastes' behavior during extrusion from core samplers. The first objective of the study was to quantify waste behavior during horizontal extrusion by documenting the extrusion behavior of simulants with known strengths; the second was to estimate the strength of actual waste based on these simulant standards.

Results showed a reproducible extrusion behavior for bentonite clay and kaolin/Ludox® simulants over strengths ranging from 30 to 6,500 Pa. The extrusion behavior changed distinctively with variations in strength, forming the basis for creating visual standards. The extrusion behavior was documented with both video recordings and still images. Based on these visual standards, strength estimates were made for wastes from DSTs 241-SY-103, 241-AW-101, and 241-AN-103 and SST 241-S-102. These strength estimates were compared to available in-tank ball rheometer data and laboratory data, and the estimates from horizontal extrusions generally agreed within a factor of two with the ball rheometer data, which is acceptable accuracy for use in bubble retention models.

Acknowledgments

A number of staff at the Hanford Site have contributed to success of this project, and the authors would like to thank these individuals for their important contributions. Scot Rassat assisted with the simulant preparation and apparatus assembly. Mike Powell provided information on the earlier work on horizontal extrusion behavior, and this project evolved from a series of early conversations with Mike. In addition, Mike has been instrumental in developing and characterizing both the bentonite clay and kaolin/Ludox simulants used in this study. Bertrand Griffin II and Ray Akita of Hanford's 222-S hot cell facility were very helpful over the past two years in making available the video recordings of the core extrusions. And the editorial assistance of Sheila Bennett and Karen Mercer have been truly valuable.

Contents

Figures

Tables

1.0 Introduction

The Hanford Site has 149 single-shell tanks (SSTs) and 28 double-shell tanks (DSTs) containing radioactive wastes that are complex mixes of radioactive and chemical products. Some of these wastes are known to generate mixtures of flammable gases, including hydrogen, nitrous oxide, and ammonia. Nineteen of these SSTs and six of the DSTs have been placed on the Flammable Gas Watch List because they are known or suspected, in all but one case, to retain these flammable gases (Hanlon 1995). Because these gases are flammable, their retention and episodic release pose a number of safety concerns. Understanding the physical mechanisms and waste properties that contribute to the retention and release of these gases will help to resolve the flammable gas safety issues (Johnson et al. 1997).

The waste strength plays a central role in both the mechanisms of bubble retention and bubble release (Rassat et al. 1997; Gauglitz et al. 1995, 1996; Stewart et al. 1996b). While recent in-situ measurements with the ball rheometer (Stewart et al. 1996a; Meyer et al. 1997) have provided results for five of the DSTs, waste strength measurements are typically not available for any of the SSTs nor for those DSTs that have not been characterized with the ball rheometer. Accordingly, a method is needed to estimate waste strength from readily available data or observations.

Over the past few years, video recordings of the extrusion of actual waste materials from core samplers have been routinely collected in the Hanford's 222-S hot cell facility. These extrusions are performed horizontally. It is apparent from these images that a wide range of waste behavior is exhibited during the extrusions. In a recent study, Powell et al. (1995) discussed the behavior of simulants during horizontal extrusion and presented a theoretical relationship for determining the tensile strength from horizontal extrusion. The extrusion behavior for a simulant composed of kaolin clay and colloidal silica (Ludox®) was consistent with the assumptions used in developing the relationship. In contrast, the behavior of bentonite clay simulants was inconsistent with the assumptions (shear failure rather than tensile failure), so it was considered inappropriate to use the derived relationship for calculating tensile strengths. Still, it was apparent that the bentonite extrusion behavior depended on the simulant strength, but the relationship was more complicated. While a more sophisticated theoretical relationship can be developed, empirical observations can also be used to establish a quantitative relationship between extrusion behavior and strength. This is the approach used in this work. While this empirical relationship is perhaps more easily developed, it will always have a more qualitative character than an appropriate theoretical relationship.

2.0 Objective and Scope

The overall purpose of this study was to develop a method to obtain strength estimates for actual wastes from observations of the wastes during extrusion from core samplers. The first objective of the study was to quantify waste behavior during horizontal extrusion by documenting the extrusion behavior of simulants with known strengths. If the results showed a reproducible extrusion behavior over a wide range of strengths, and if the extrusion behavior changed distinctively with variations in strength, then visual standards could be created for estimating strengths. The second objective of this study was to estimate the strength of actual waste based on these simulant standards. Finally, the strength estimates were compared with the existing data.

3.0 Experimental Methods and Materials

Two substantially different simulants were used in this study to reflect the wide variety of mechanical behavior typical of wastes from SSTs and DSTs. Bentonite clay simulants with a range of strengths were chosen to mimic the plastic, drooping behavior of many wastes. Kaolin/Ludox simulants were selected because they show brittle failure rather than plastic deformation, and because they mimic the behavior of a number of wastes as well. Ludox is a trade name for colloidal silica. The experimental apparatus and methods and the details of the simulants are described in the following sections.

The behavior differences between the bentonite and kaolin/Ludox simulants can be related to the particle scale behavior within these colloidal dispersions (Powell et al. 1995). For the bentonite clay simulants, the strength results from the attractive and repulsive colloidal forces (van der Waals and electrostatic) between the particles. If macroscopic deformation causes the particles to change position, the interparticle interactions are reestablished within seconds. When the bentonite simulant is extruded horizontally, it tends to bend or droop with significant plastic deformation before failure. In contrast, the strength of the kaolin/Ludox simulants is dominated by the gel structure of the colloidal silica, and these interparticle interactions are reestablished over periods of several days. If macroscopic deformation causes the silica gel structure to break, the material fails quickly without showing much plastic deformation. When the kaolin/Ludox simulant is extruded horizontally it tends to extrude as a stiff cylinder; then it breaks somewhat cleanly and without excessive bending, in contrast to the bentonite simulants.

3.1 Extrusion Apparatus and Method

Figure 3.1 shows the apparatus for extruding the simulants. The apparatus was assembled so that the dimension of the horizontal extrusions would mimic those of the actual waste. It consists primarily of a 2.5 cm inner diameter (i.d.) by 60 cm long tube containing the simulant, a plunger attached to a threaded rod, and a variable speed motor. The tube dimensions are essentially identical to the typical 1-in. i.d. by 19-in.-long core sampler. When operated, the threaded rod pulls on the tube and exposes, or extrudes, the simulant. At its fastest speed, the extrusion rate was approximately 4.5 cm/min, which was somewhat slower than the typical extrusions of actual waste. The extrusions were recorded with a video camera and recorder. The experiment consists of filling the tube with the simulant, assembling the apparatus, then extruding the material while recording the extrusion behavior. Particular attention was paid to recording the initial extrusion behavior and the overall shape of the simulants during the extrusion.

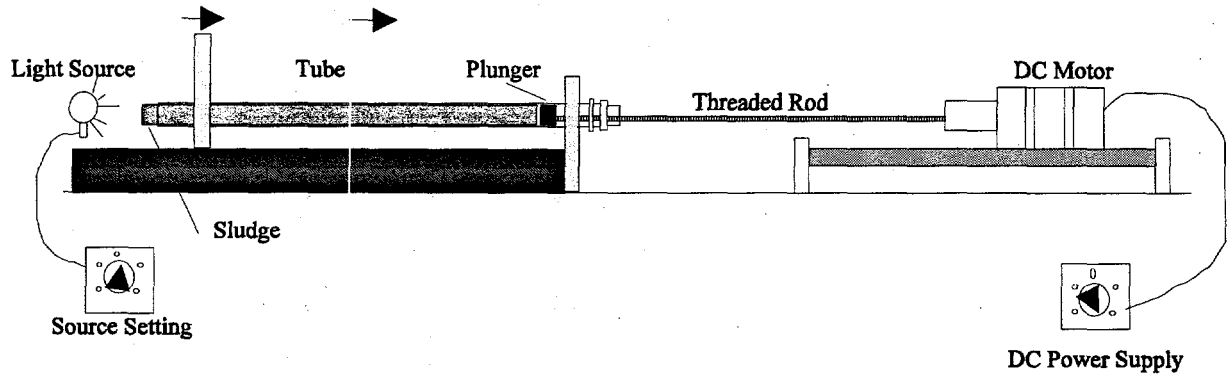

Figure 3.1. Horizontal Extrusion Apparatus

3.2 Bentonite Clay Simulants

Bentonite clay simulants were prepared by mixing dry bentonite clay (Bighorn bentonite) with deionized water following the technique described by Gauglitz et al. (1996). The desired amount of water was added to a mixer bowl, and then the bentonite was added over a 15- to 45-minute period, depending on the amount to be added. The mixture was readily combined with a standard kitchen-type mixer, and the sides of the mixer bowl required repeated scraping to ensure a uniform mixture. Previously, the shear strength (shear vane measurement) of a number of specific bentonite mixtures had been measured and reported (Gauglitz et al. 1996), and we used these specific mixtures. Table 3.1 gives the mixtures prepared and their respective shear strengths.

3.3 Kaolin/Ludox Simulants

The kaolin/Ludox simulant is a mixture of kaolin clay powder; Ludox HS-30, which is a readily available colloidal silica dispersion; NaCl; and deionized water. The shear strengths of these simulants are predictably controlled with the set time and concentrations of Ludox and salt (Powell et al. 1995).[(a)] To make these simulants, the water was first added to the mixer bowl, then the NaCl was added and mixed until dissolved. Ludox HS-30 was then added, followed by the kaolin. Extra care was taken when conducting experiments with this simulant. The simulant was pourable immediately after mixing, so it was added directly to the extruding tube and stored upright. Each simulant was allowed to set in the tube for the amount of time needed to reach its required shear strength. The simulant could not be disturbed during this

---

(a) In a letter report entitled, *Development of a Double-Shell Slurry Physical Simulant to be used for Pilot Scale Sludge Mobilization Testing,* (November 1987, GAW-02088) GA Whyatt (PNNL) presented detailed experimental results showing the progression of shear strengths with time and the dependence of Ludox and salt concentrations.

Table 3.1. Bentonite Clay Mixtures

Wt% Clay	Shear Strength (Pa)	Bentonite Powder (g)	H_20 Added (g)
12.50	31	186	1,302
13.75	67	206	1,292
15.00	147	227	1,286
15.62	217	237	1,280
16.25	323	247	1,273
16.88	463	258	1,270
17.50	656	269	1,268
18.75	1,040	290	1,257
20.75	1,660	326	1,245
24.00	2,660	385	1,219
27.25	3,670	385	1,196

period because disturbance of the material would likely have disrupted the formation of the silica gel structure and the subsequent extrusion results. Table 3.2 shows the kaolin/Ludox mixtures used and the shear strengths reported in the Whyatt letter report for these specific mixtures and set times.

Table 3.2. Kaolin/Ludox Mixtures

Shear Strength (Pa)	Set Time (hr)	Wt% Kaolin Powder	Wt% Water	Wt% Ludox HS-30	Wt% NaCl
625	5.5	47.7	28.8	22.8	0.7
1,000	7.0	47.5	27.3	24.5	0.7
1,600	22.0	47.7	28.8	22.8	0.7
2,500	52.5	47.6	28.3	23.4	0.7
4,000	71.0	47.3	26.4	25.6	0.7
6,500	68.5	46.6	22.8	29.9	0.7

4.0 Extrusion Results for Simulants

Results have been obtained for the general shape of bentonite simulants during extrusion and the length of the initial extruded segments at the point of failure for both bentonite and kaolin/Ludox simulants. Figures 4.1 through Figure 4.11 show the observed extrusion behavior for the bentonite clays with strengths ranging from 31 to 3670 Pa. For the weakest materials tested, small slices seemed to slip off the end of the tube. As the simulant became stronger, say a few hundred Pa, the waste showed a drooping behavior where the waste slumped sharply to the table beneath the extrusion tube. For the strongest simulants tested, the extruded simulant becomes a progressively straighter bar. In summary, the simulant results in Figures 4.1 to 4.11 show a reproducible extrusion behavior that changes distinctively with variations in strength, indicating that these images can be the basis of visual standards for estimating strength. The extrusion behavior was documented with both video recordings and the presented still images; copies of the video recordings are available.[(a)]

An alternative method for estimating strength is based on measurements of the initial extrusion behavior of the simulants. In a previous study, Powell et al. (1995) discussed the results of a force analysis of the extruded waste as a cantilevered beam. The force analysis gave the following relationship between the length of the piece that breaks free, L, and the tensile strength S_t:

$$S_t = \frac{64(M_h)^2(g)}{\pi^2(D_t)^5(\rho_{sludge})} + \frac{8(M_h)(g)}{3\pi(D_t)^2}\frac{[0.925]}{[1.04]}$$

where

$$M_h = \rho_{sludge}(L)(A)$$

and D_t is the extrusion tube diameter, A is the tube cross sectional diameter, ρ_{sludge} is the sample density, and g is the gravitational acceleration. This equation makes a number of simplifying assumptions, including that the material shows no appreciable bending before failure and that brittle failure rather than plastic failure occurs.

(a) Contact PA Gauglitz at Pacific Northwest National Laboratory, Richland, Washington, 99352.

The initial extrusion lengths at failure are useful for determining strength when the breaks occur in a consistent fashion. The kaolin/Ludox simulants showed brittle failure, in general agreement with the assumptions of the force balance given above, and this behavior mimics some important actual waste extrusions. Table 4.1 gives the initial extrusion length for the kaolin/Ludox simulants tested and the strengths estimated from these lengths. While the bentonite clay simulants did not show brittle failure, experimental results for the initial extrusion length were also collected for this material. Table 4.2 gives the lengths and calculated strengths based on these lengths for the different bentonite simulants. Figure 4.12 shows the relationship between these lengths and both the measured shear strengths (labeled Data) and tensile strengths calculated from the initial extrusion lengths (labeled Theory). While the comparison shows a significant difference between these strengths, these results also demonstrate a reproducible extrusion behavior that changes distinctively with variations in strength, again indicating that extrusion images can be the basis of visual standards for estimating strength. The initial extrusion behavior was also documented with video recordings, and Figures 4.13 through 4.17 show still images for the kaolin/Ludox simulants; Figures 4.18 through 4.23 show the behavior for the bentonite simulants.

Table 4.1. Data for Kaolin/Ludox Horizontal Extrusions

Shear Strength (Pa)	Initial Extrusion Length (m)	Density (kg/m^3)	Calculated Tensile Strength (Pa)
625	0.046	1,516	5,293
1,000	0.056	1,519	7,813
1,600	0.056	1,516	7,798
2,500	0.058	1,517	8,505
4,000	0.064	1,521	10,026
6,500	0.071	1,528	12,559

Table 4.2. Data for Bentonite Clay Horizontal Extrusions

Shear Strength (Pa)	Initial Extrusion Length (m)	Density (kg/m^3)	Calculated Tensile Strength (Pa)
31	0.008	1,078	144
67	0.017	1,087	562
147	0.025	1,096	1,250
217	0.028	1,100	1,500
323	0.033	1,104	2,070
463	0.043	1,109	3,649
656	0.051	1,113	4,760
1040	0.053	1,122	5,270
1660	0.066	1,137	8,890
2660	0.081	1,162	12,400
3670	0.091	1,189	16,000

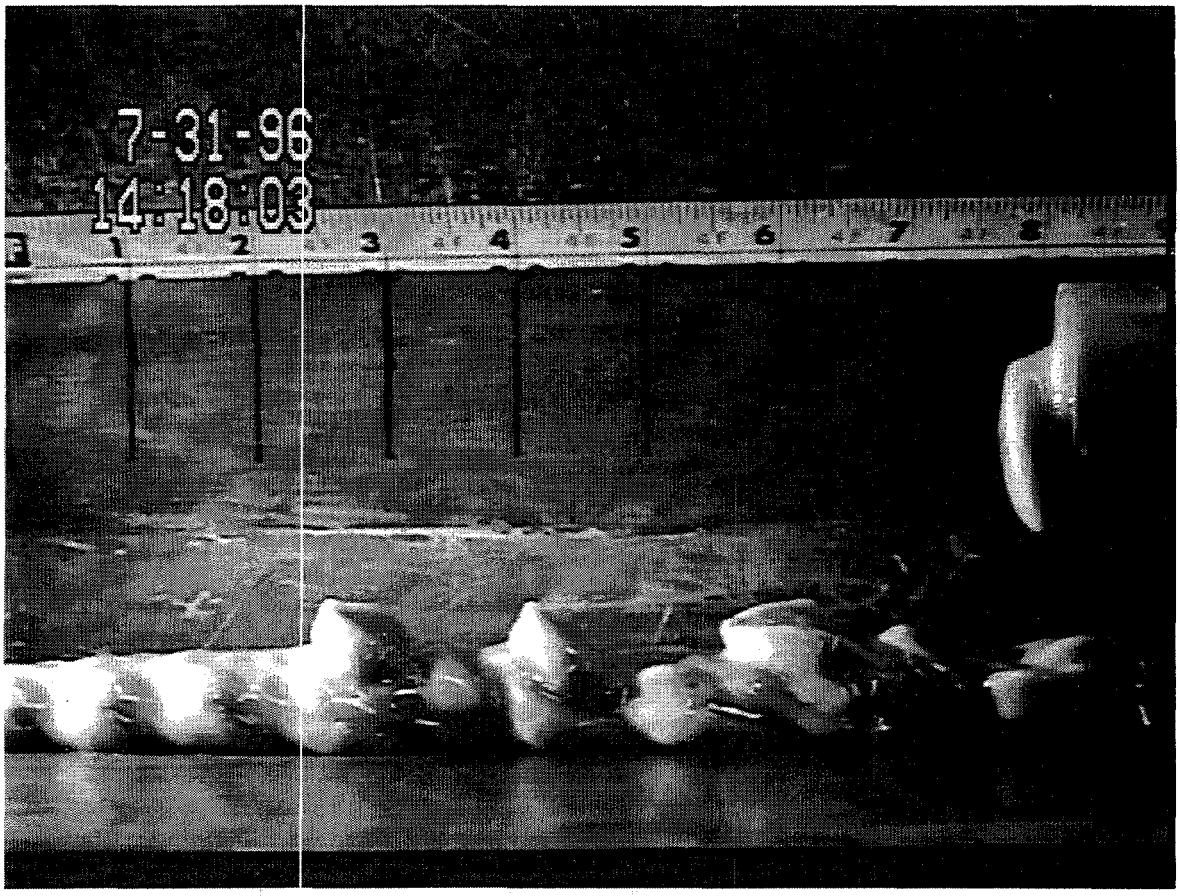

Figure 4.1. Extrusion Behavior for 31 Pa Bentonite Clay Simulant

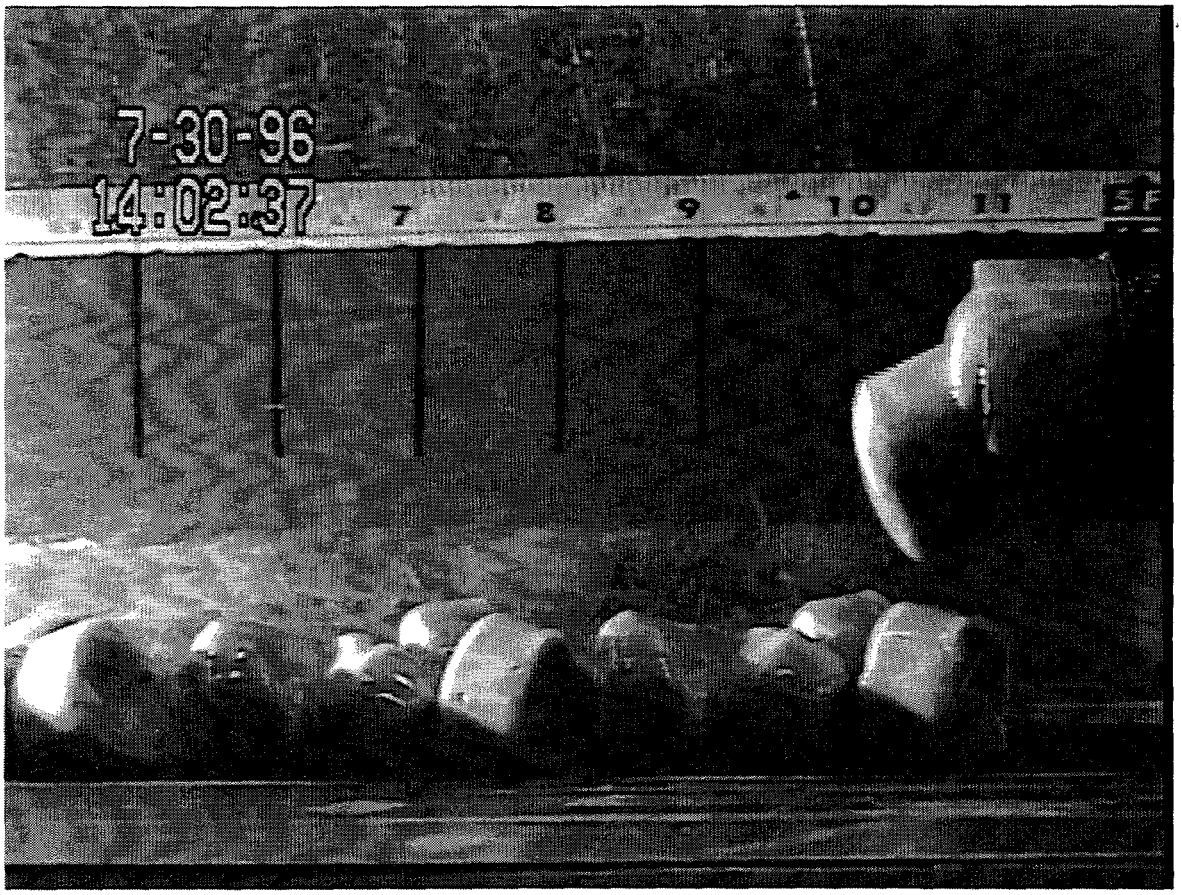

Figure 4.2. Extrusion Behavior for 67 Pa Bentonite Clay Simulant

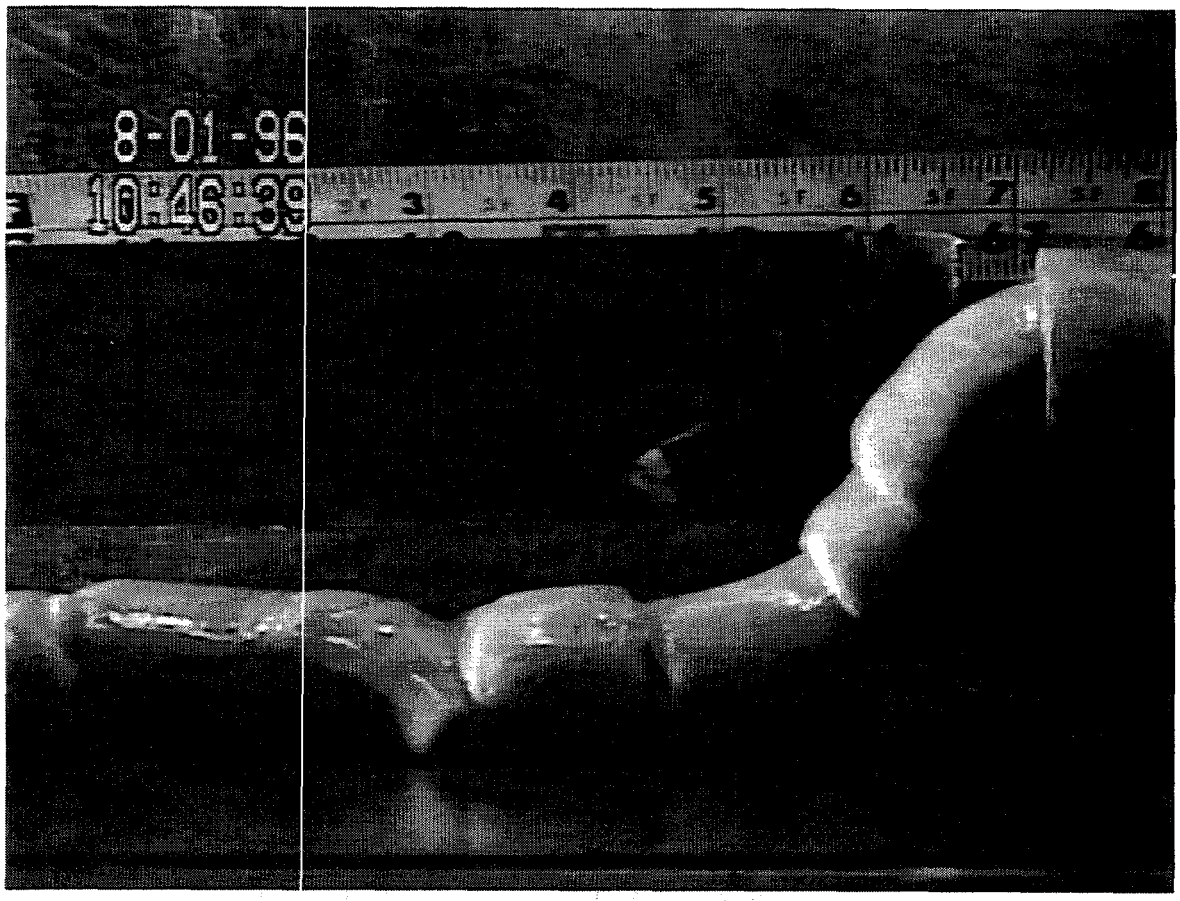

Figure 4.3. Extrusion Behavior for 147 Pa Bentonite Clay Simulant

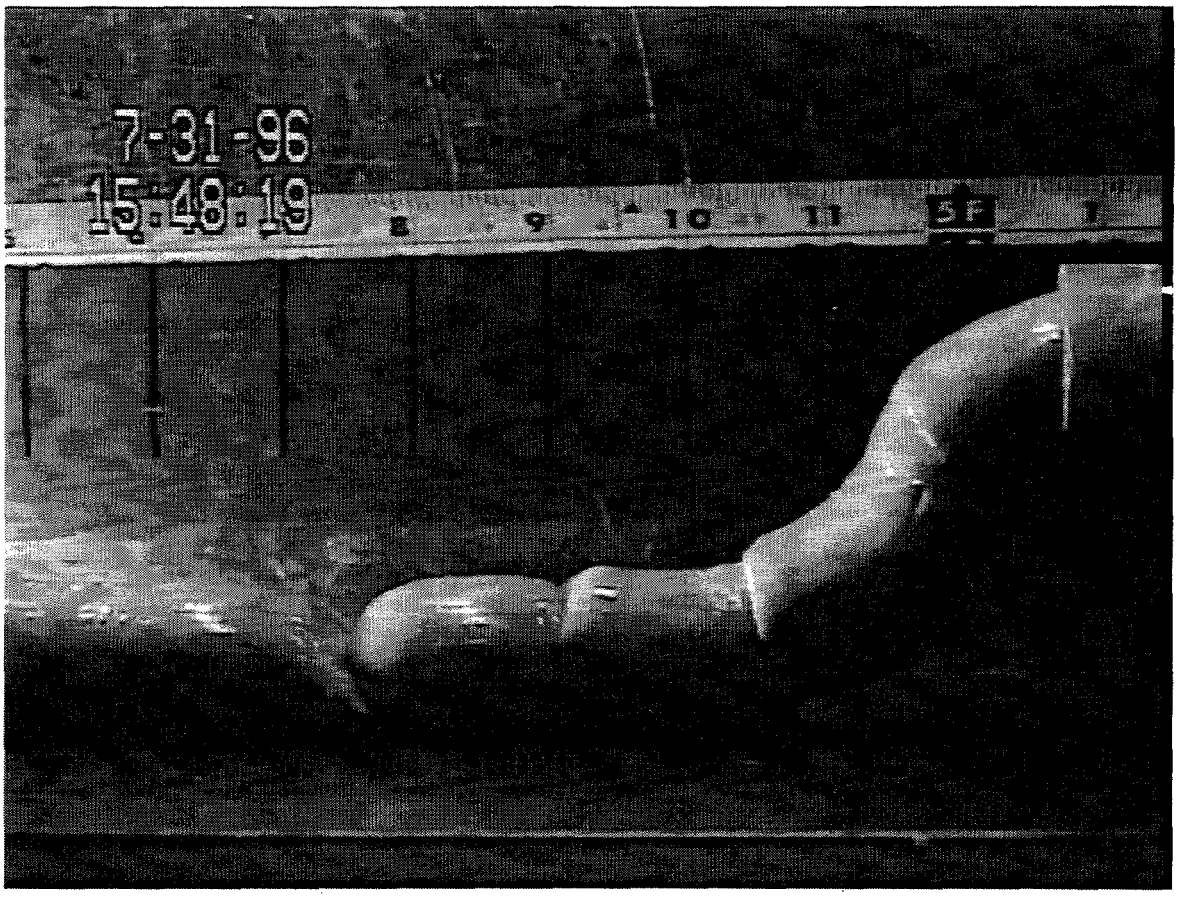

Figure 4.4. Extrusion Behavior for 217 Pa Bentonite Clay Simulant

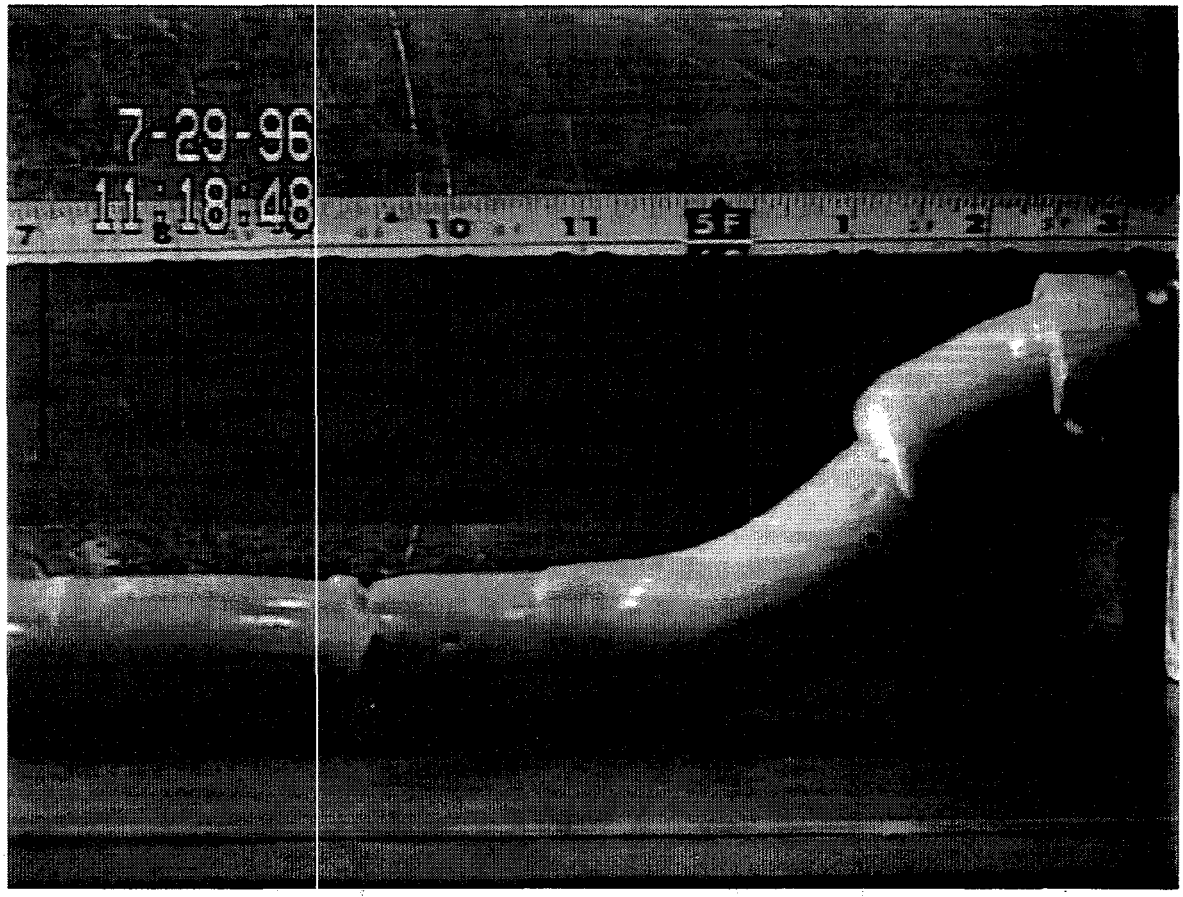

Figure 4.5. Extrusion Behavior for 323 Pa Bentonite Clay Simulant

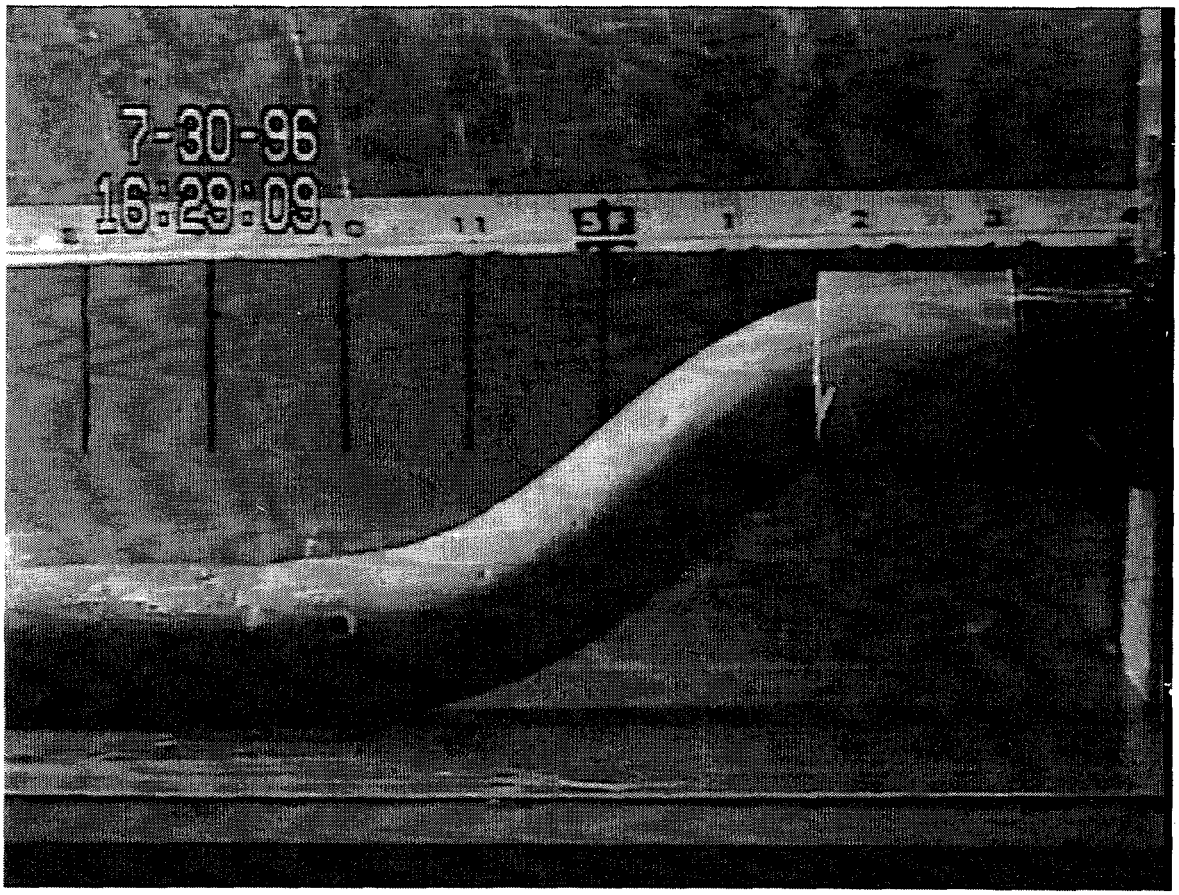

Figure 4.6. Extrusion Behavior for 463 Pa Bentonite Clay Simulant

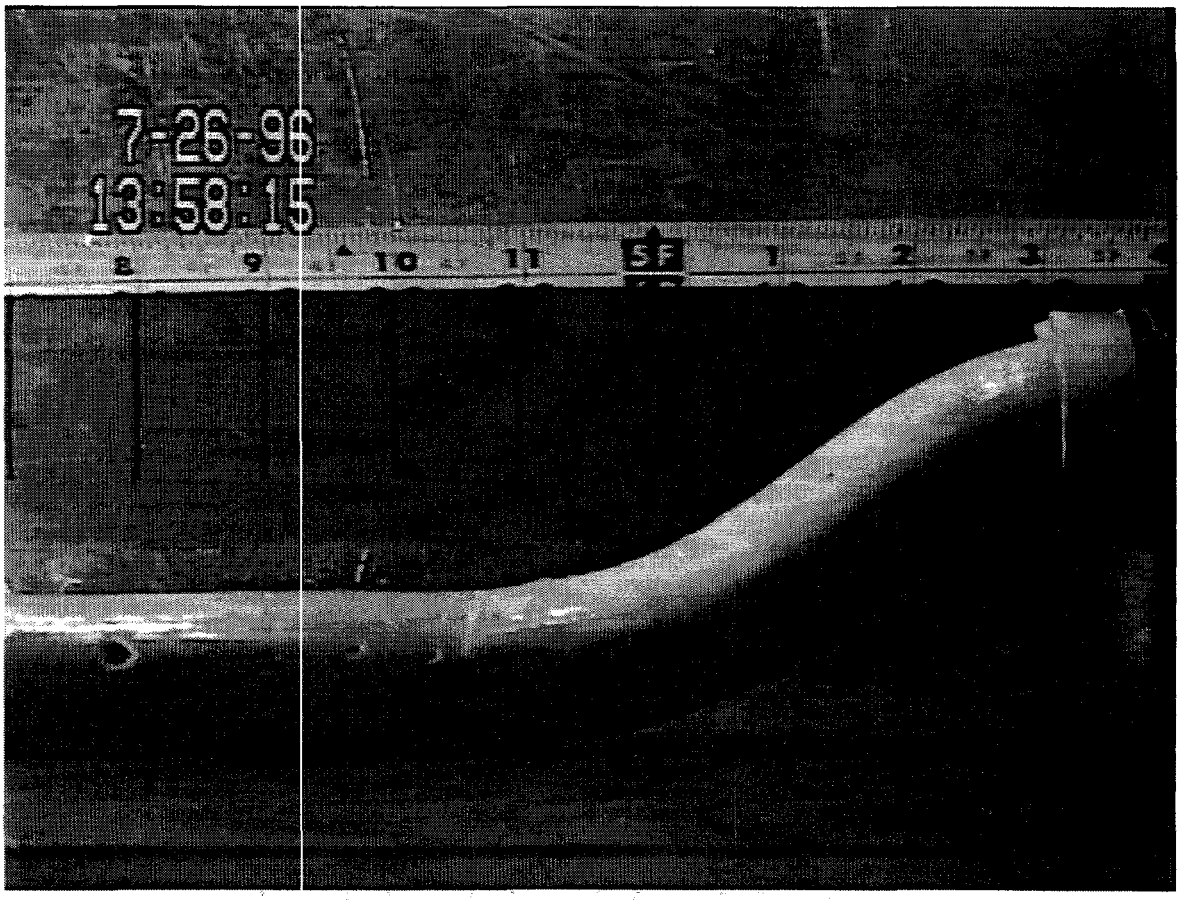

Figure 4.7. Extrusion Behavior for 656 Pa Bentonite Clay Simulant

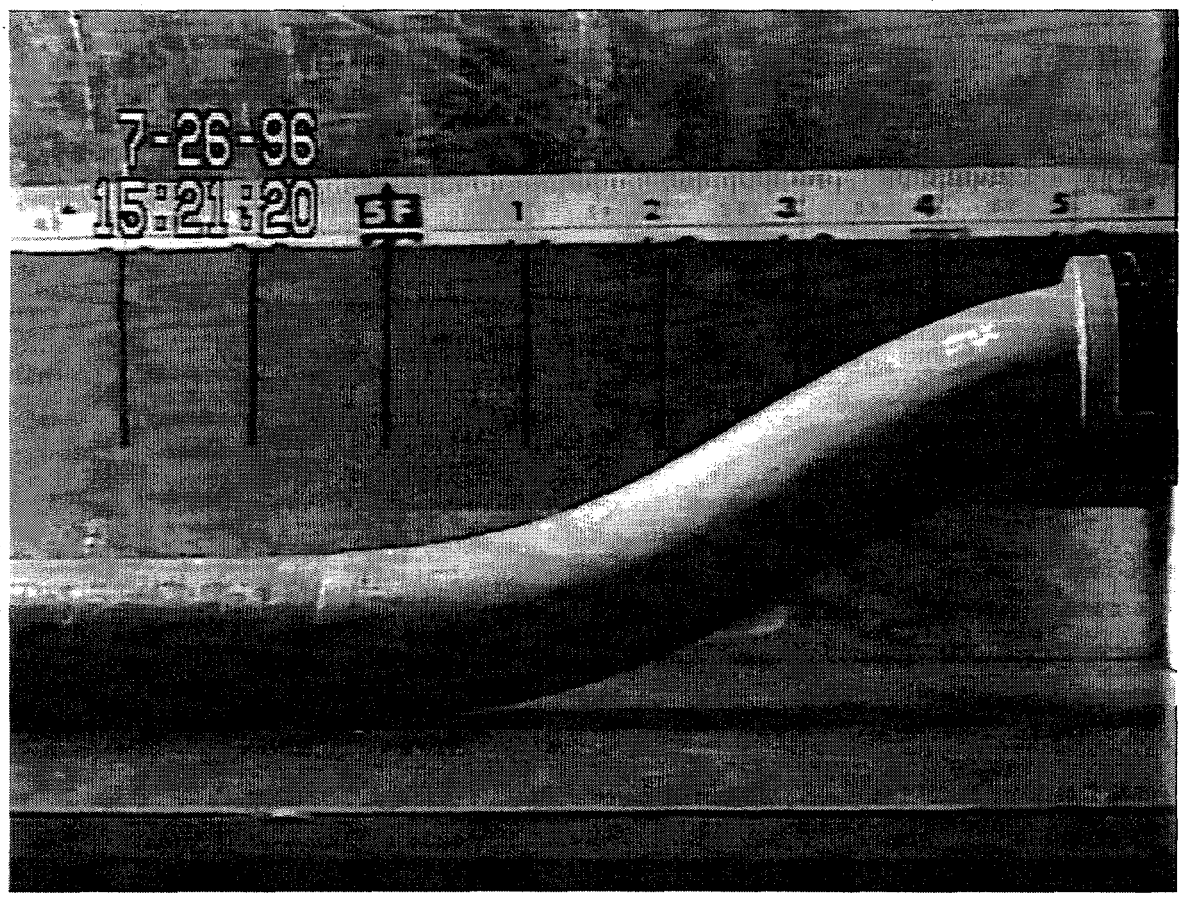

Figure 4.8. Extrusion Behavior for 1,040 Pa Bentonite Clay Simulant

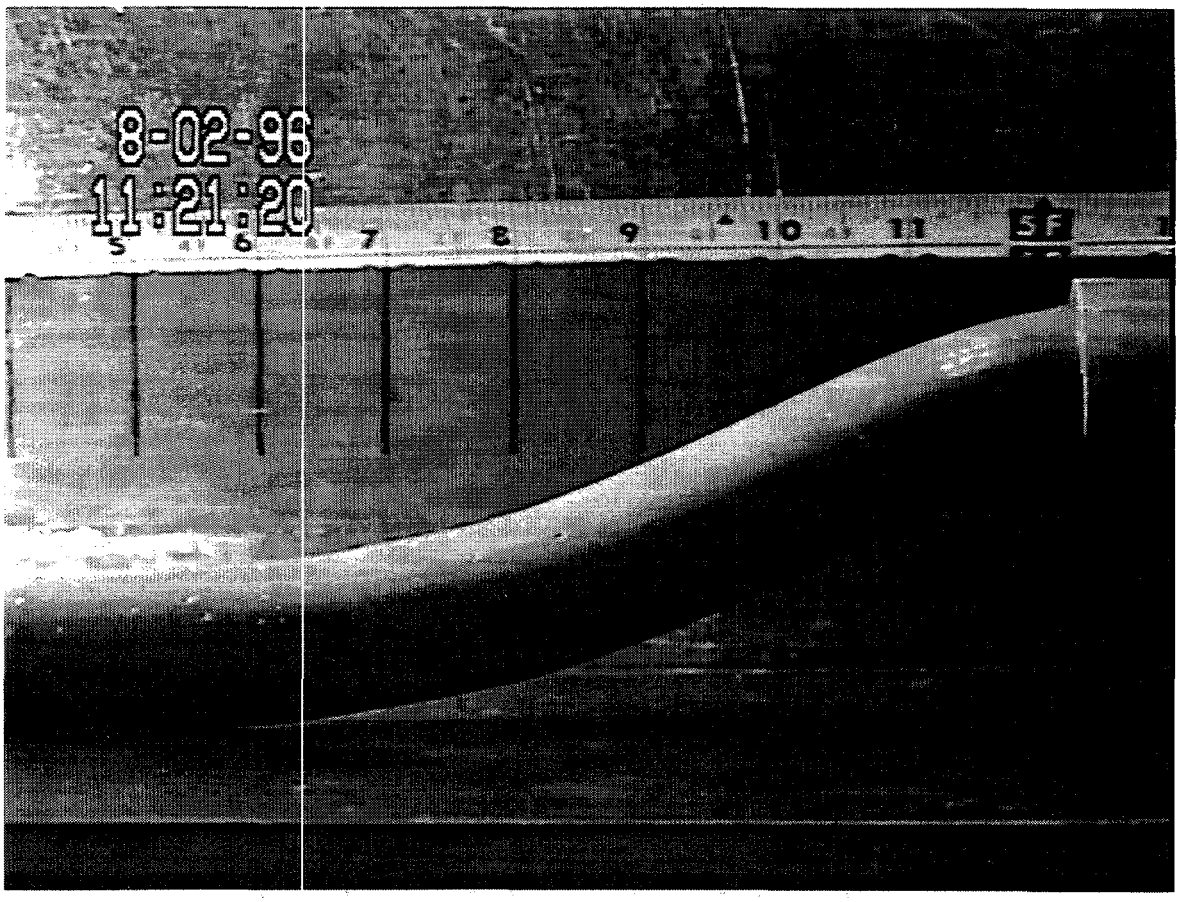

Figure 4.9. Extrusion Behavior for 1,660 Pa Bentonite Clay Simulant

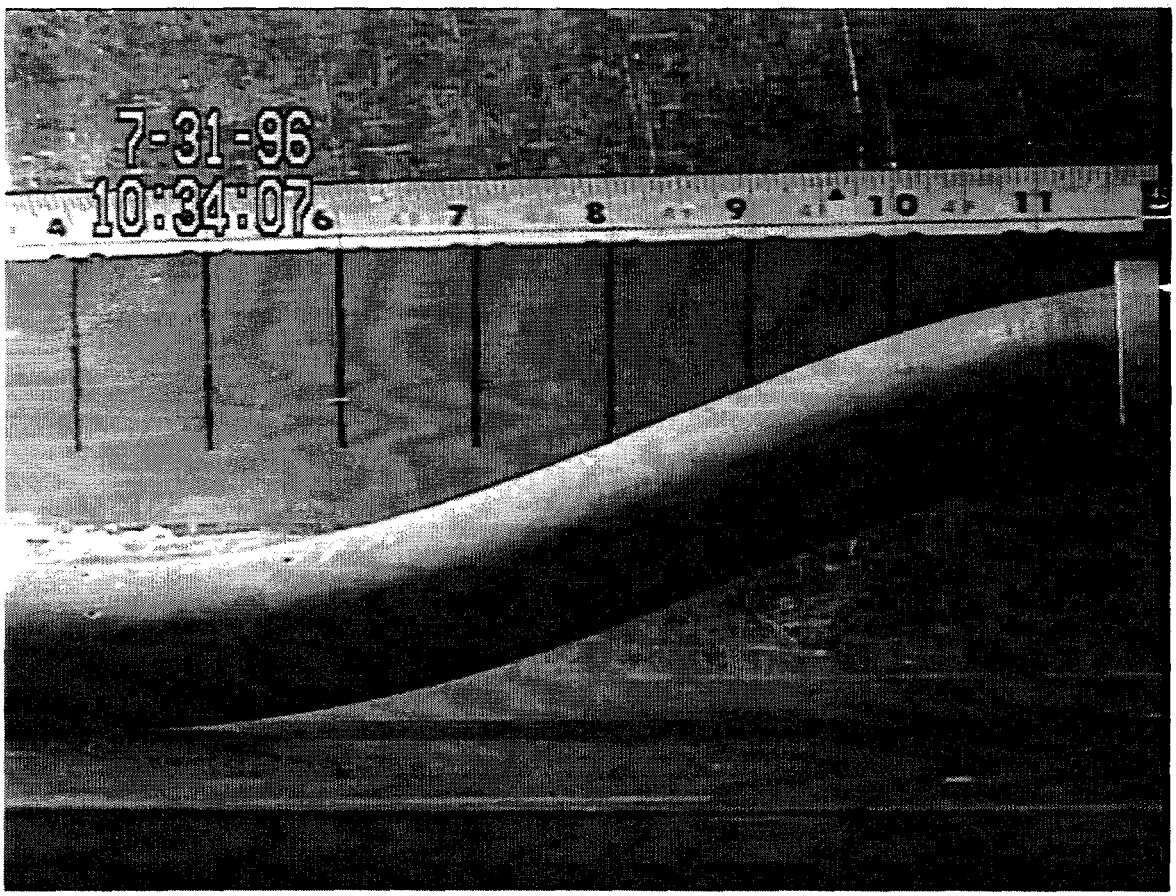

Figure 4.10. Extrusion Behavior for 2,660 Pa Bentonite Clay Simulant

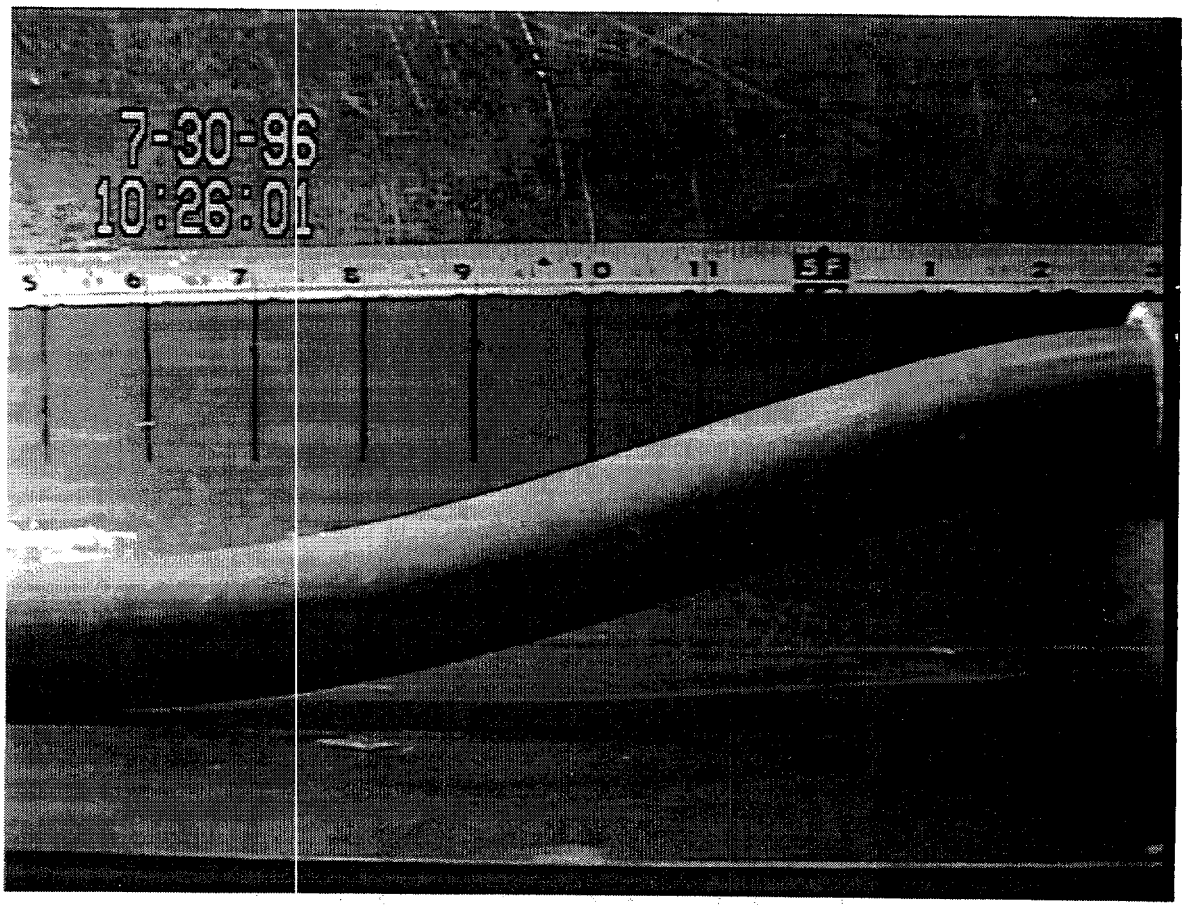

Figure 4.11. Extrusion Behavior for 3,670 Pa Bentonite Clay Simulant

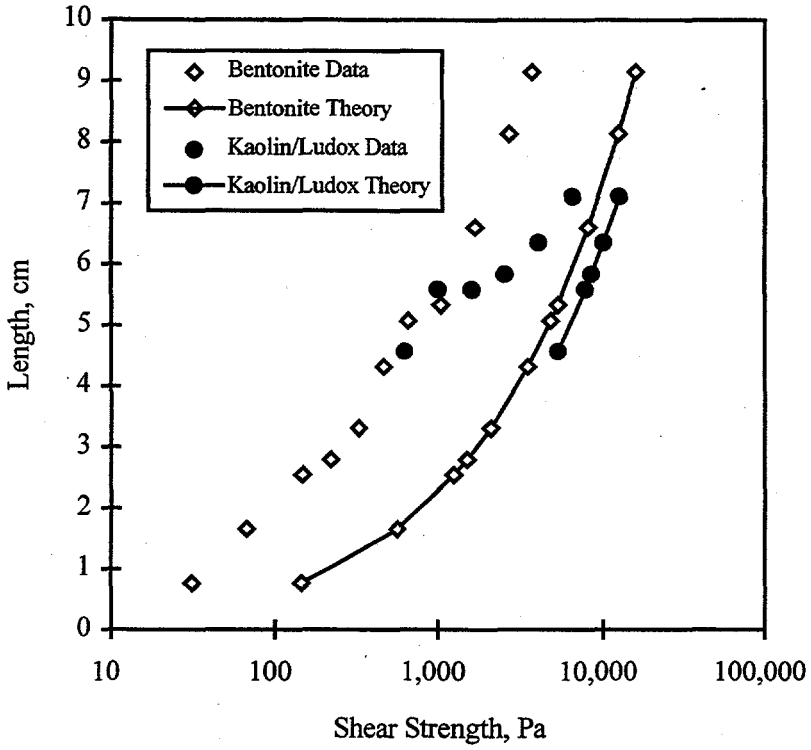

Figure 4.12. Comparison of Shear Strength and Tensile Strength Calculated from Initial Extrusion Lengths

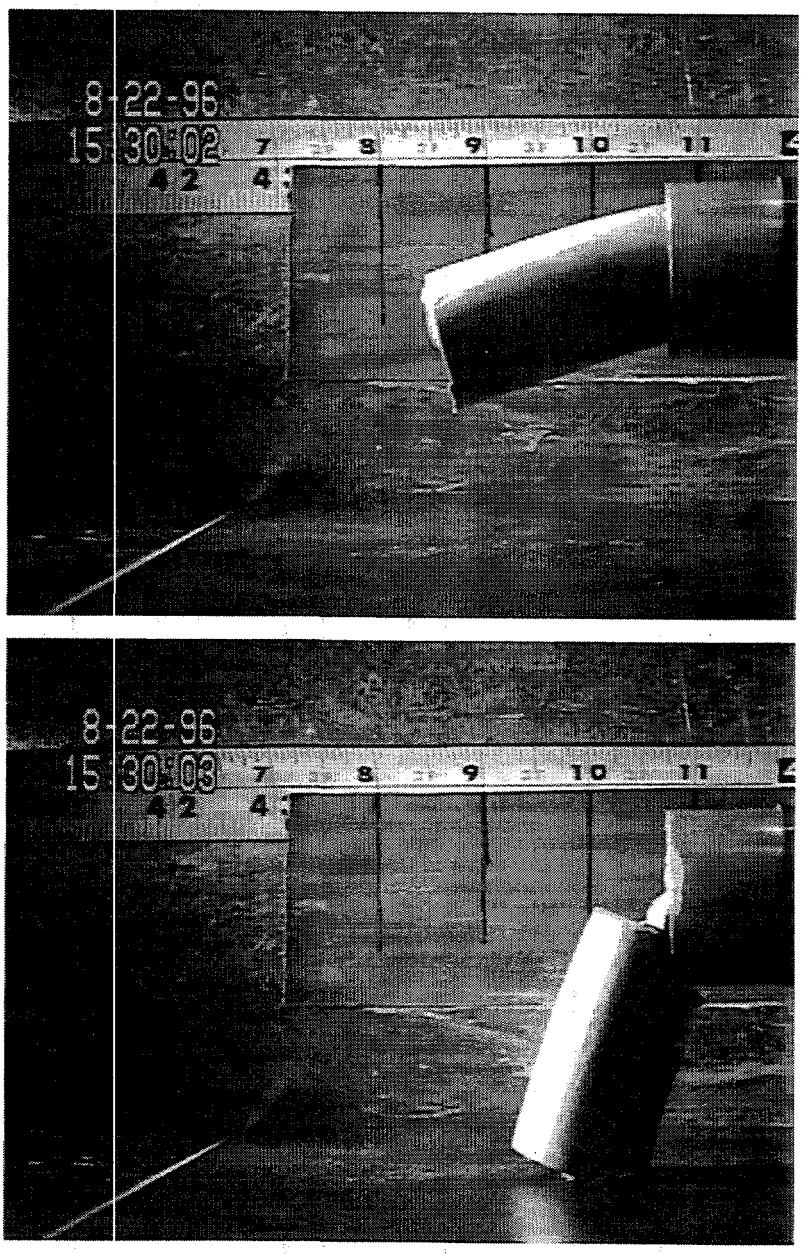

Figure 4.13. Initial Extrusion Behavior for 625 Pa Kaolin/Ludox Simulant

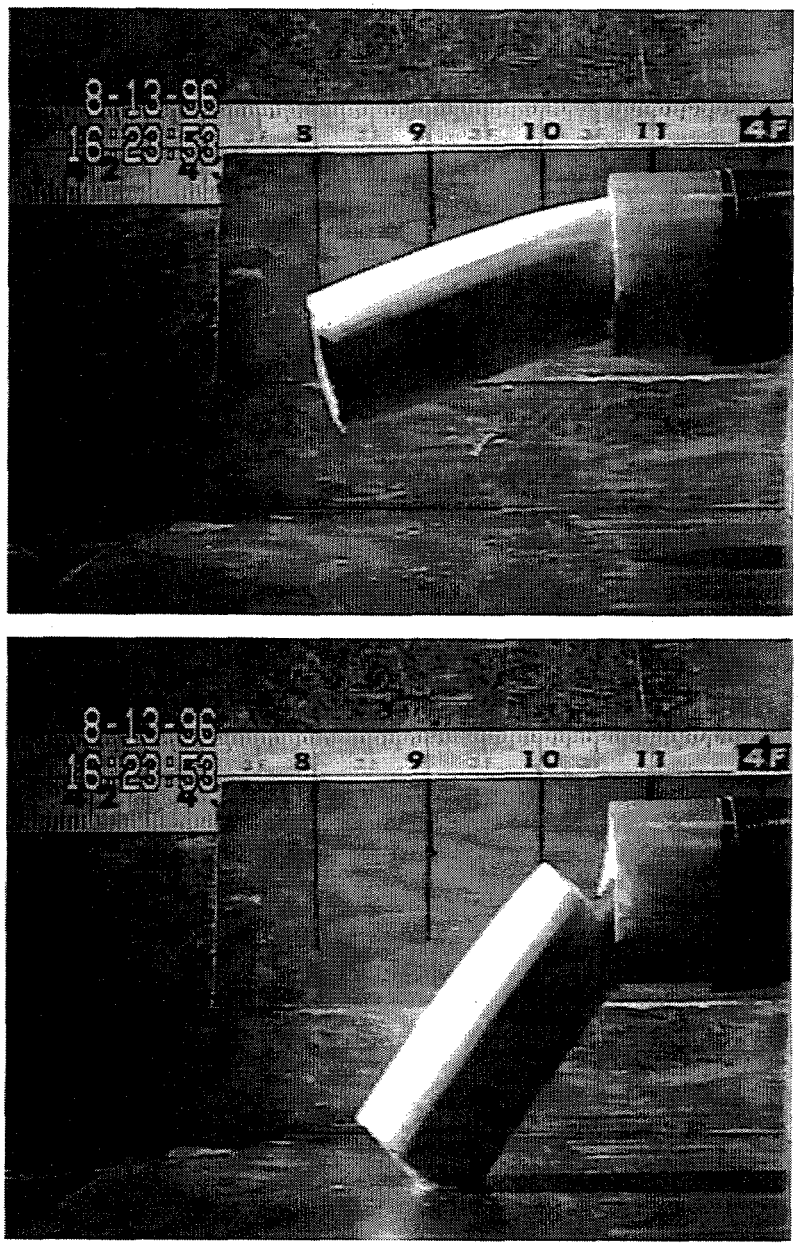

Figure 4.14. Initial Extrusion Behavior for 1,000 Pa Kaolin/Ludox Simulant

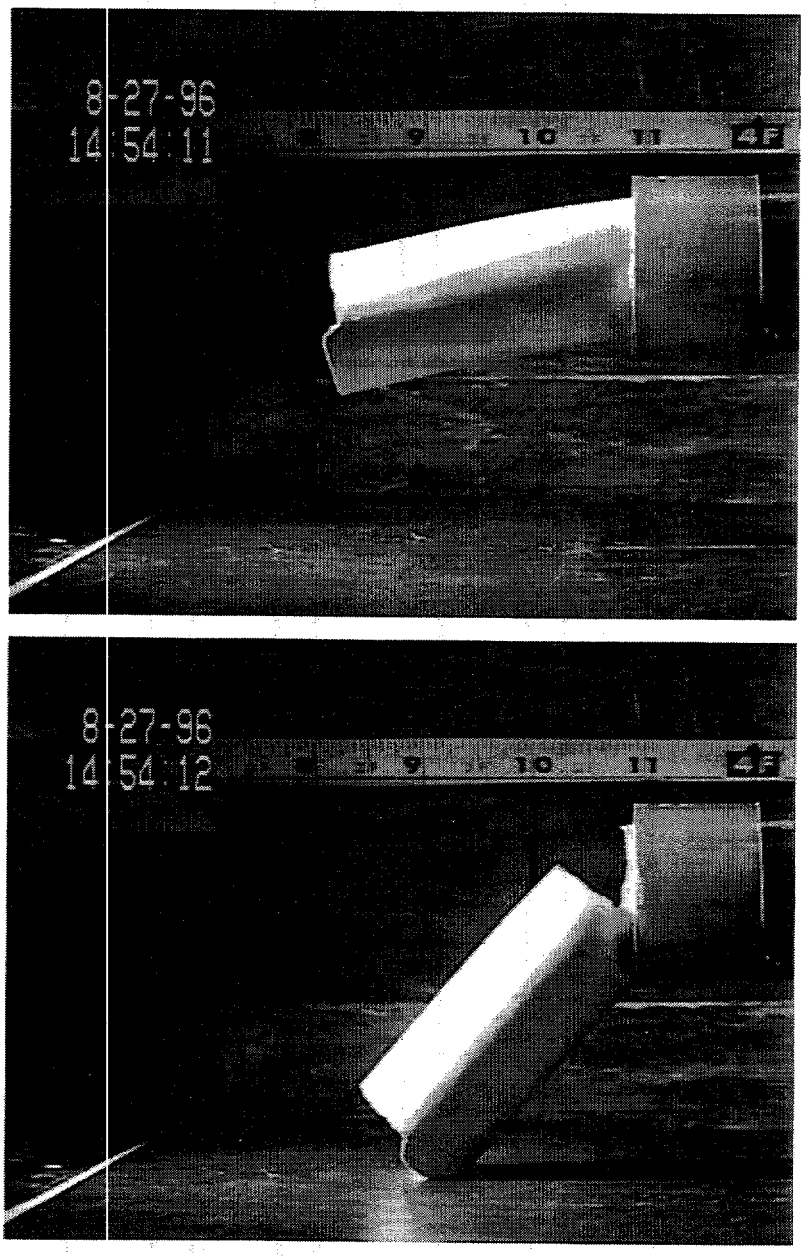

Figure 4.15. Initial Extrusion Behavior for 1,600 Pa Kaolin/Ludox Simulant

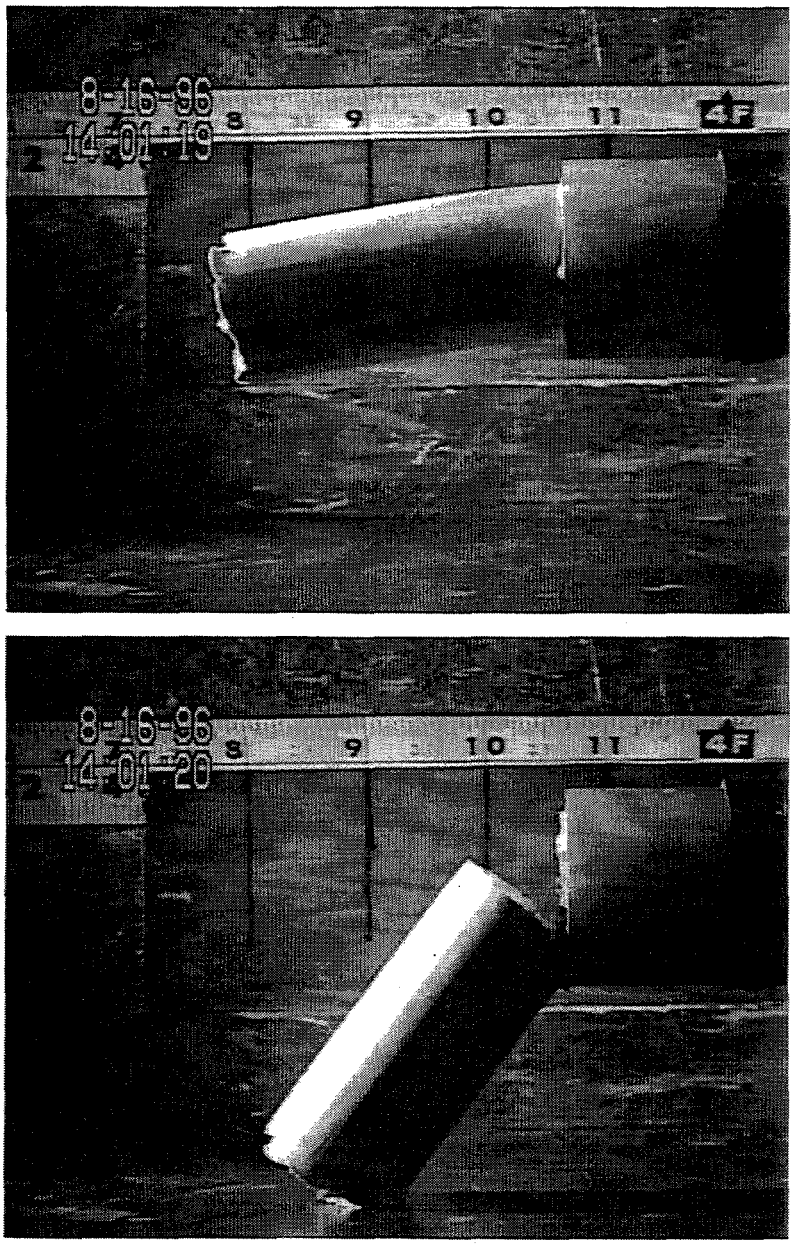

Figure 4.16. Initial Extrusion Behavior for 2,500 Pa Kaolin/Ludox Simulant

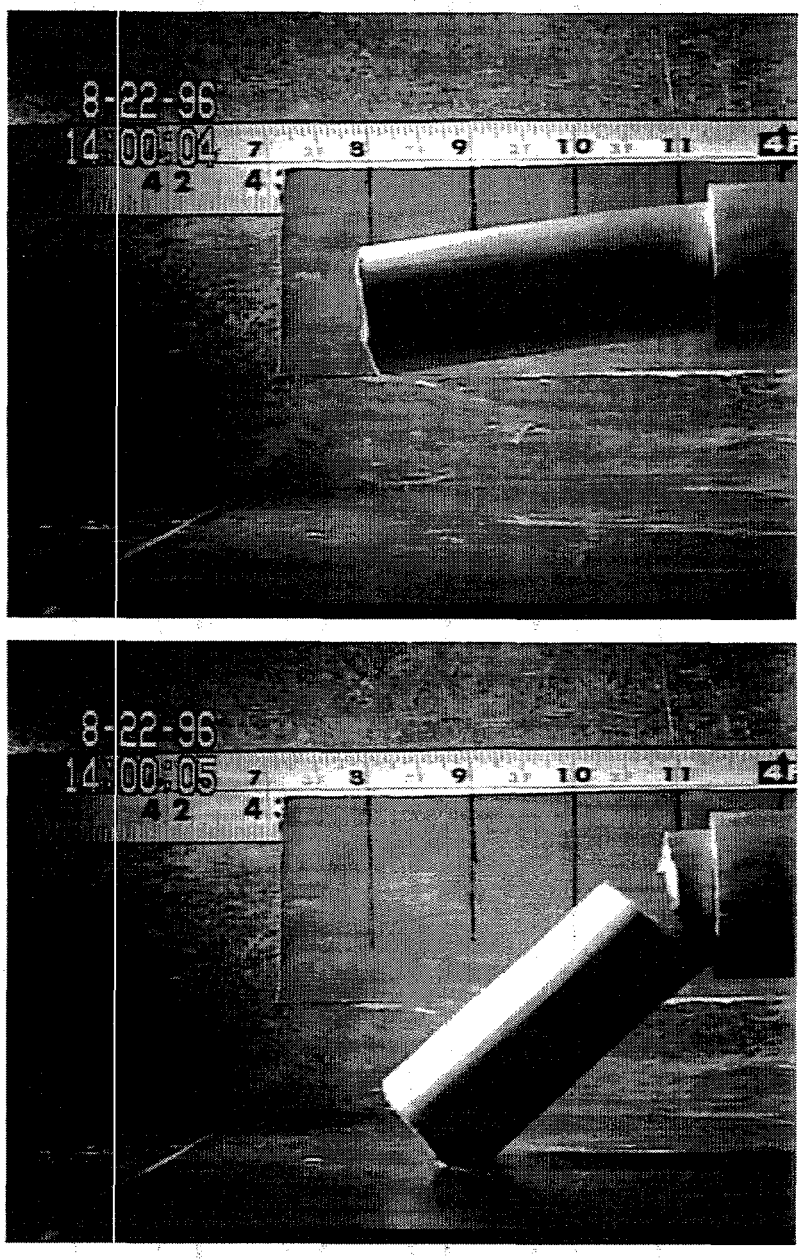

Figure 4.17. Initial Extrusion Behavior for 4,000 Pa Kaolin/Ludox Simulant

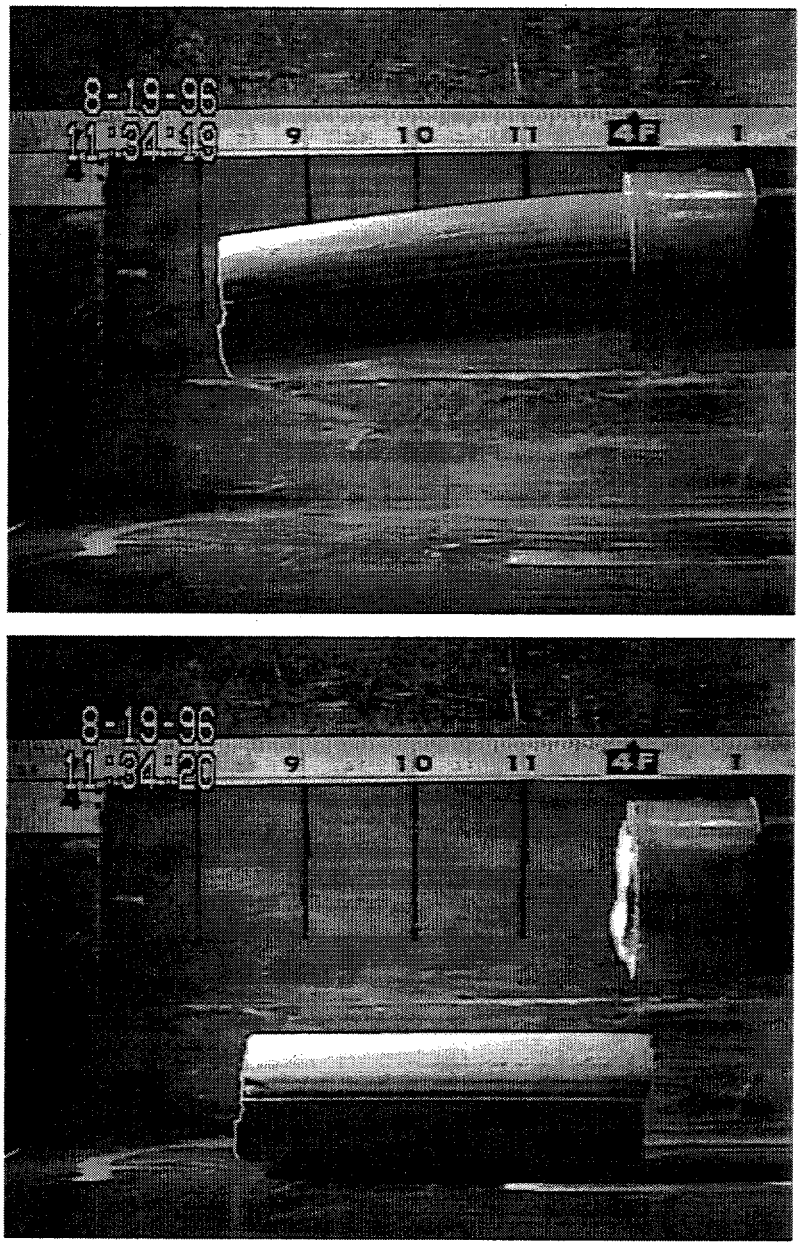

Figure 4.18. Initial Extrusion Behavior for 6,500 Pa Kaolin/Ludox Simulant

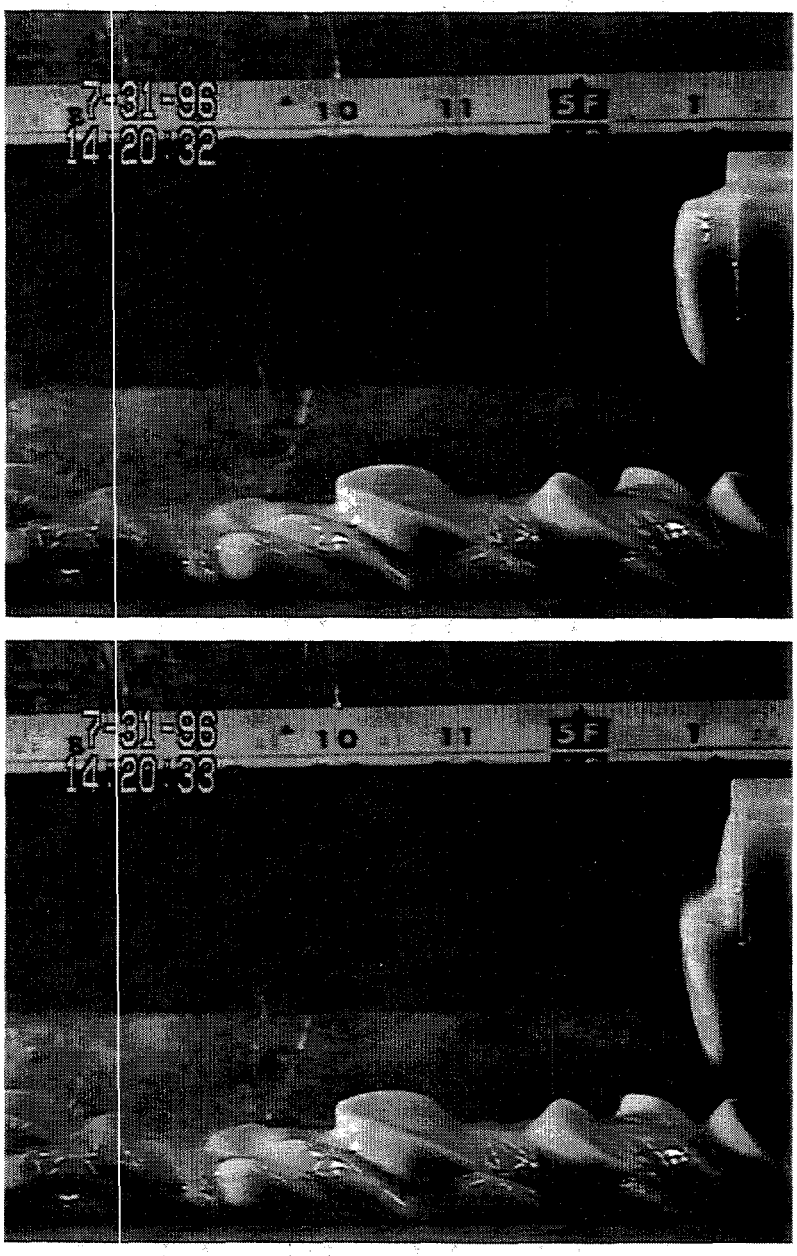

Figure 4.19. Initial Extrusion Behavior for 31 Pa Bentonite Clay Simulant

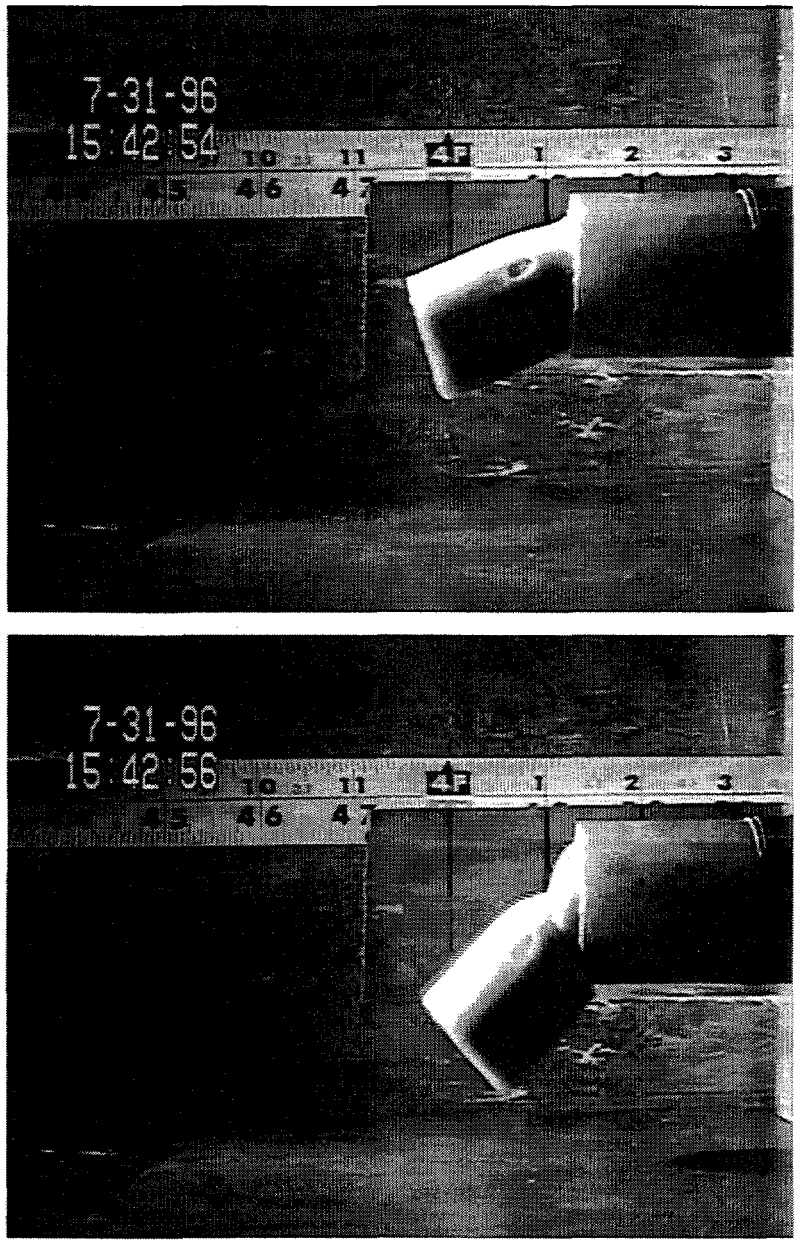

Figure 4.20. Initial Extrusion Behavior for 217 Pa Bentonite Clay Simulant

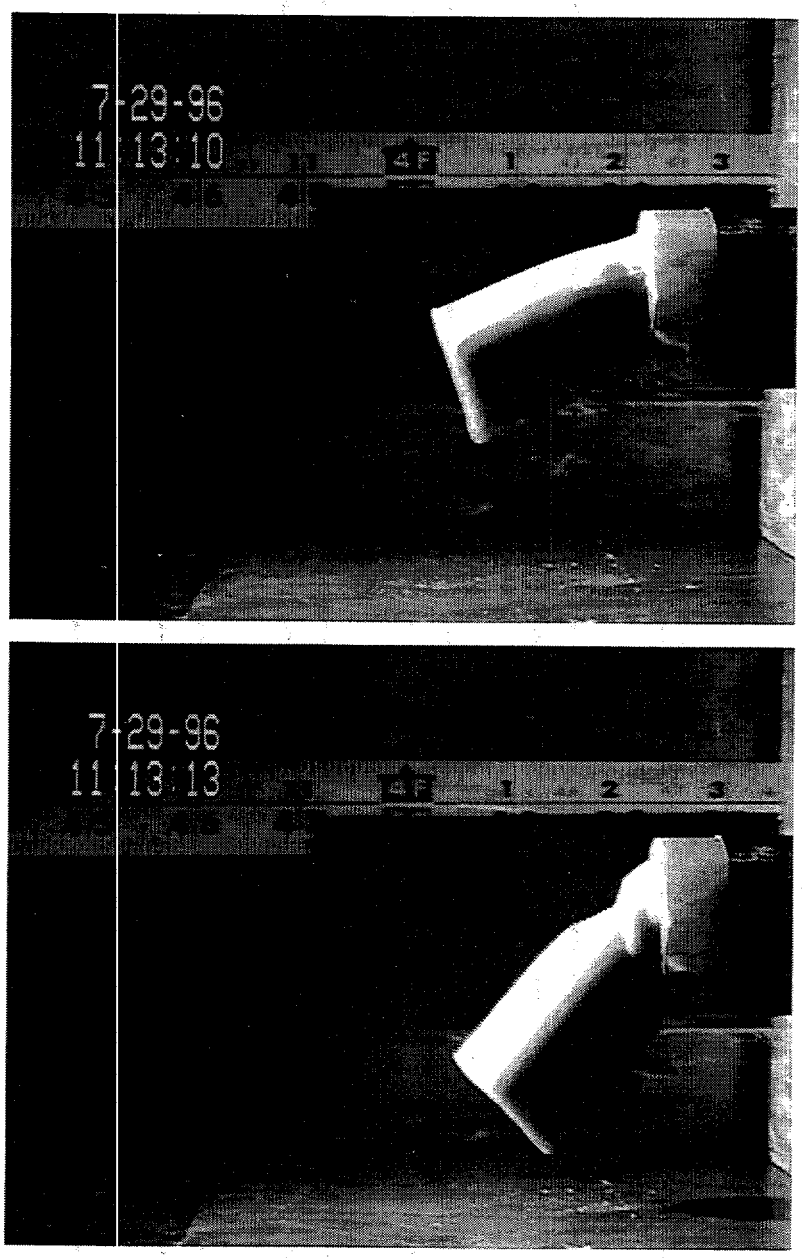

Figure 4.21. Initial Extrusion Behavior for 323 Pa Bentonite Clay Simulant

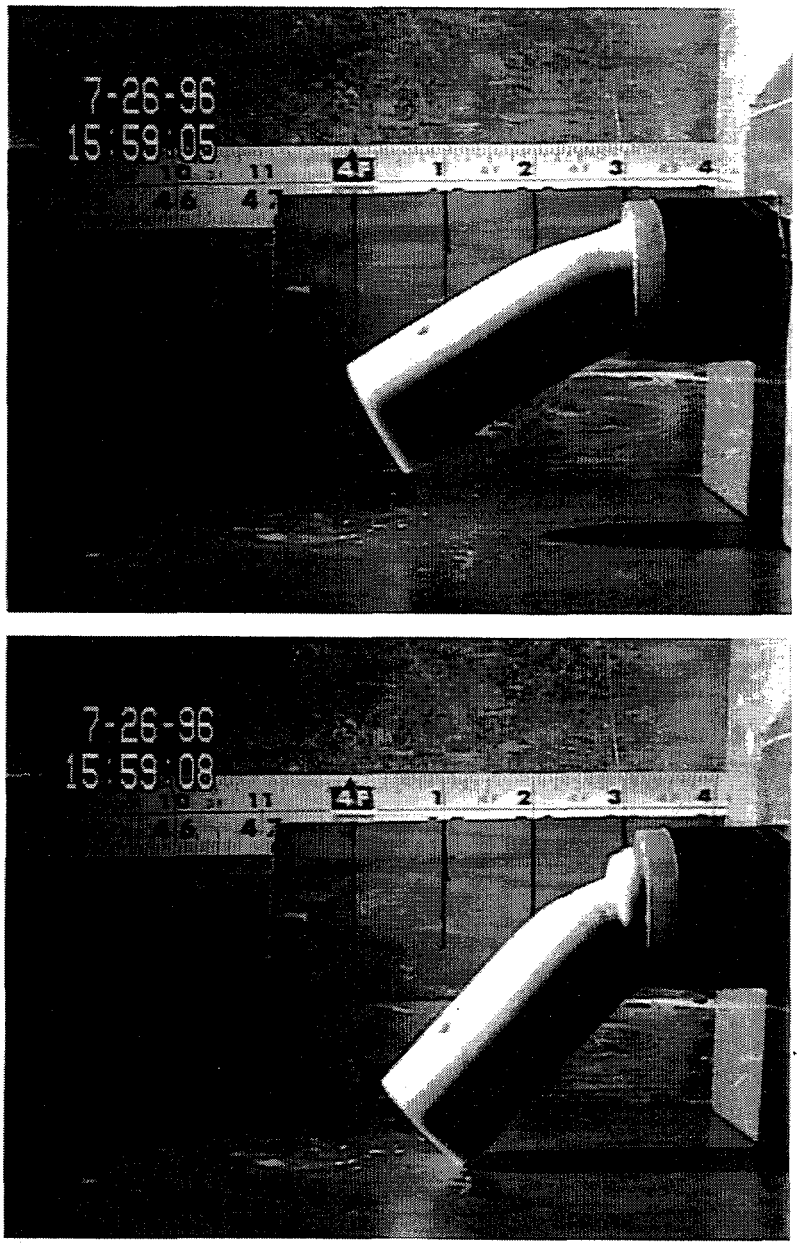

Figure 4.22. Initial Extrusion Behavior for 1,040 Pa Bentonite Clay Simulant

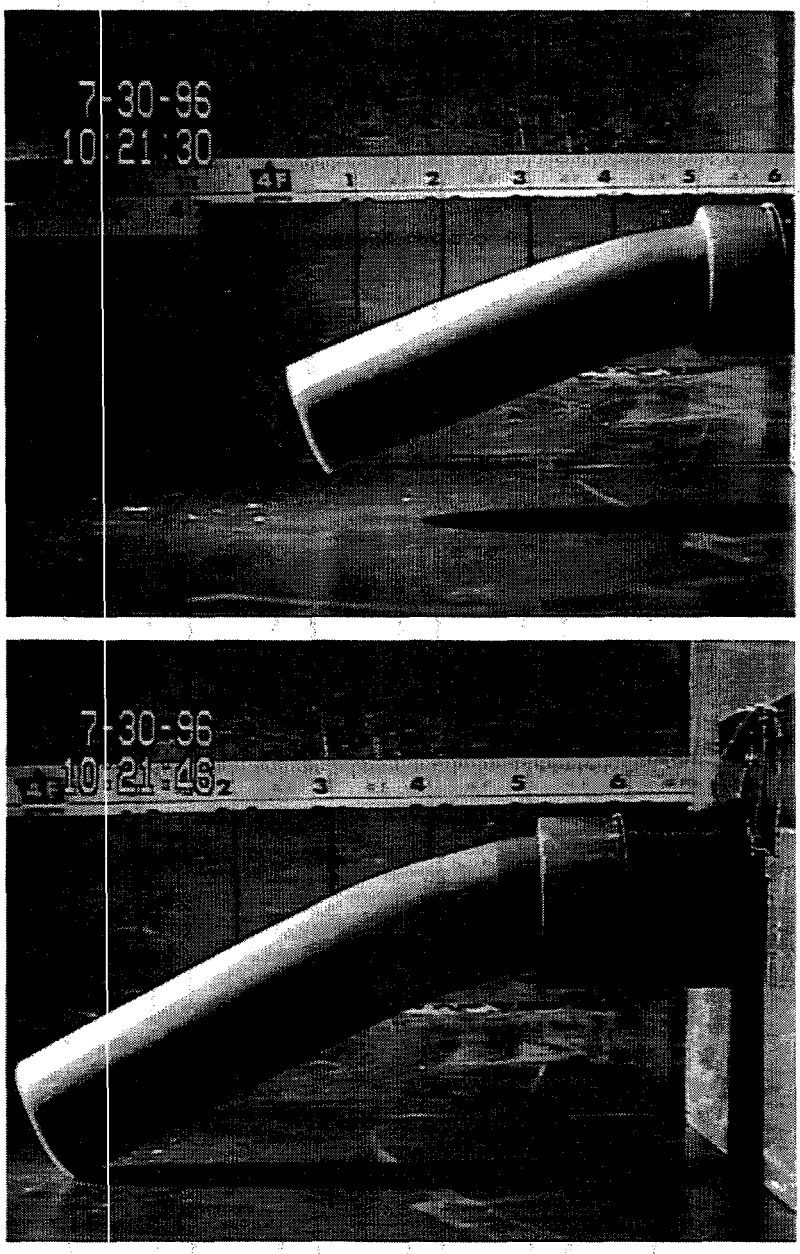

Figure 4.23. Initial Extrusion Behavior for 3,670 Pa Bentonite Clay Simulant

5.0 Strength Estimates for Actual Wastes

In this section, the strengths of actual wastes are estimated with the visual standards relating strength and the horizontal extrusion behavior presented in Section 4. Videos of core extrusions were obtained, and strength estimates were determined for wastes from DSTs 241-SY-103, 241-AW-101, and 241-AN-103 and SST 241-S-102. These particular tanks have been the focus of gas bubble retention and release studies with actual waste (Gauglitz et al. 1996; Rassat et al. 1997). In these studies, the waste strength is an important parameter used in classifying bubble retention mechanisms. For each of these tanks, the strength estimates have been compared with available in-tank ball rheometer data and laboratory shear vane data. The results for each tank are summarized in the following sections together with selected still images from the core extrusions.

In general, differences in strength results from these methods, particularly the laboratory shear vane and ball rheometer tests, are not unexpected because these techniques measure distinct properties in the same material. For the shear vane and ball rheometer measurements, a few-fold difference is not unexpected (Heath 1987). Shear strength is determined from the peak torque required to rotate a shear vane at low shear rate in the undisturbed solid-like material. On the other hand, the ball rheometer method is a viscosity measuring technique in which the yield stress in a fluid is evaluated from measurements at a series of shear rates (ball velocities). In general, the shear strength (shear vane) is expected to be different, and greater, than the yield stress (Heath 1987). The discrepancy will be enhanced in materials where a considerable solid-like structure has developed prior to disturbance by a shearing force in a shear strength test.

5.1 Strength Estimates for SY-103

Strength estimates were determined from core extrusions of segments from SY-103, core 62. Table 5.1 summarizes the strength estimates and Figure 5.1 presents a comparison of these strength estimates, yield stress determined with the in-tank ball rheometer for risers 22A and 17C (Meyer et al. 1997), and laboratory shear vane measurements.[a] Meyer et al. (1997) also noted that, when the waste completely supported the ball, which was toward the bottom of the tank, waste yield stress was at least 900 Pa. For SY-103, the elevation where the ball was supported was 102 cm for riser 17C and 105 cm for riser 22A. Selected images of the core extrusions for each segment are shown in Figures 5.2 to 5.6. Core 62 from SY-103 had 15 segments, and the approximate elevation of each segments was determined by assuming the lowest segment began at the tank bottom and each segment was 19 inches long.

(a) Laboratory shear vane measurements of shear strength at 40°C were reported by Bredt et al. in a September 1995 letter report entitled, *Effects of Dilution on the Physical, Rheological, and Chemical Properties of Tanks 241-SY-103 Waste* (PNLMIT-092995).

The images of the cores extrusions for SY-103 are similar to the drooping behavior exhibited by the bentonite simulants. Accordingly, the strength estimates for SY-103 are based on comparisons of the extrusion behavior of the actual waste with the bentonite behavior. The comparison between the different measurement techniques given in Figure 5.1 shows reasonable agreement between the ball rheometer data and the estimates from the horizontal extrusions. The shear vane results are clearly higher. A variety of factors, such as sample handling and settling or the inherent difference in measurement techniques, may contribute to the shear vane data being higher; the specific cause of this difference is not known.

Table 5.1. SY-103 Segment Shear Strength Estimations

Segment	Elevation at Segment Midpoint (cm)	Estimation Using Bentonite Simulants (Pa)	Estimation Using Kaolin/Ludox Simulants (Pa)
10[(a)]	290	30-70	-
11	240	100-200	-
12	193	150-250	-
13	145	300-450	-
14	97	150-250	-

(a) Did not see entire extrusion.

5.2 Strength Estimates for AN-103

Strength estimates were determined from core extrusions of segments from AN-103, core 167. Table 5.2 summarizes the strength estimates, and Figure 5.7 compares these estimates and yield stress determined with the in tank ball rheometer for risers 1B and 16B (Meyer et al. 1997) and laboratory shear vane measurements on essentially undisturbed samples reported by Rassat et al. (1997). Meyer et al. (1997) also noted that when the waste completely supported the ball, which was toward the bottom of the tank, waste yield stress was at least 900 Pa. For AN-103, the elevation where the ball was supported was 227 cm for riser 16B and 158 cm for riser 1B. Selected images of the core extrusions for each segment are shown in Figures 5.8 to 5.12. Core 167 from AN-103 had 18 segments, and the approximate elevation of each segment was determined by assuming that the lowest segment began at the tank bottom and that each segment was 19 inches long.

Table 5.2. AN-103 Segment Shear Strength Estimations

Segment	Elevation at Segment Midpoint (cm)	Estimation Using Bentonite Simulants (Pa)	Estimation Using Kaolin/Ludox Simulants (Pa)
11	386	50-150	-
12	338	100-200	-
14	241	700-1400	-
15	193	500-1000	-
17	97	700-1400	-

The images of the cores extrusions for AN-103 are most similar to the behavior exhibited by the bentonite simulants. Accordingly, the strength estimates for AN-103 are based on comparing the extrusion behavior of the actual waste with the bentonite behavior. The comparison of the different measurement techniques given in Figure 5.7 shows reasonable agreement between the ball rheometer data and the estimates from the horizontal extrusions. Again, the shear vane data are higher, and the specific cause of this difference is not known.

5.3 Strength Estimates for AW-101

Strength estimates were determined from core extrusions of segments from AN-103, core 132. Table 5.3 summarizes the strength estimates and Figure 5.13 compares these strength estimates and yield stress determined with the in tank ball rheometer for risers 1C and 13A (Meyer et al. 1997) and laboratory shear vane measurements on undisturbed samples reported by Rassat et al. (1997). Meyer et al. (1997) also noted that when the waste completely supported the ball, which was near the bottom of the tank, waste yield stress was at least 900 Pa. For AW-101, the elevation where the ball was supported was 94 cm for riser 1C and 0 cm for riser 13A. Selected images of the core extrusions for each segment are shown in Figures 5.14 to 5.16. Core 132 from AW-101 had 22 segments, and the approximate elevation of each segments was determined by assuming the lowest segment began at the tank bottom and each segment was 19 inches long.

The images of the cores extrusions for AW-101 are most similar to the behavior exhibited by the bentonite simulants. Accordingly, the strength estimates for AW-101 are based on comparing the extrusion behavior of the actual waste to the bentonite behavior. The comparison between the different measurement techniques given in Figure 5.13 shows reasonable agreement between the ball rheometer data and the estimates from the horizontal extrusions. In this case, while the shear vane data are still higher than extrusion estimates, the difference is smaller.

Table 5.3. AW-101 Segment Shear Strength Estimations

Segment	Elevation at Segment Midpoint (cm)	Estimation Using Bentonite Simulants (Pa)	Estimation Using Kaolin/Ludox Simulants (Pa)
18	241	50-150	-
20	145	50-150	-
22	48	50-150	-

5.4 Strength Estimates for S-102

Strength estimates were determined from core extrusions of segments from S-102, core 130. Table 5.4 and Figure 5.17 summarizes these strength estimates. Data from the ball rheometer are not available for any SST, including S-102, nor are there any reported shear vane measurements for this tank to make comparisons with these estimates. Selected images of the core extrusions for each segment are shown in Figures 5.18 to 5.29. Core 130 from S-102 had 11 segments, and the approximate elevation of each segments was determined by assuming the lowest segment began at the tank bottom and each segment was 19 inches long.

The extrusion behavior for the S-102 waste was more varied that the previously discussed double shell wastes. Most of the extrusions showed failure more similar to the kaolin/Ludox simulants, though many of the extruded sections were shorter than observed for the weakest kaolin/Ludox simulant tested. In these cases, the bentonite clay initial extrusion results were used. Table 5.4 designates the visual standard used for making the estimates.

Table 5.4. S-102 Segment Shear Strength Estimations

Segment	Elevation at Segment Midpoint (cm)	Estimate Using Bentonite Simulants (Pa)	Estimate Using Kaolin/Ludox Simulants (Pa)
2	483	40-100	-
3	434	150-300	-
4	386	250-500	-
5[(a)]	338		300-1600
6a	290	100-200	-
6b	290	250-500	-
7	241	175-350	-
8a	193	-	600-1000
8b	193	-	500-1,600
9	145	1,000-1,700	-
10	97	1,000-2,000	-
11	48	-	400-800

(a) Did not see entire extrusion.

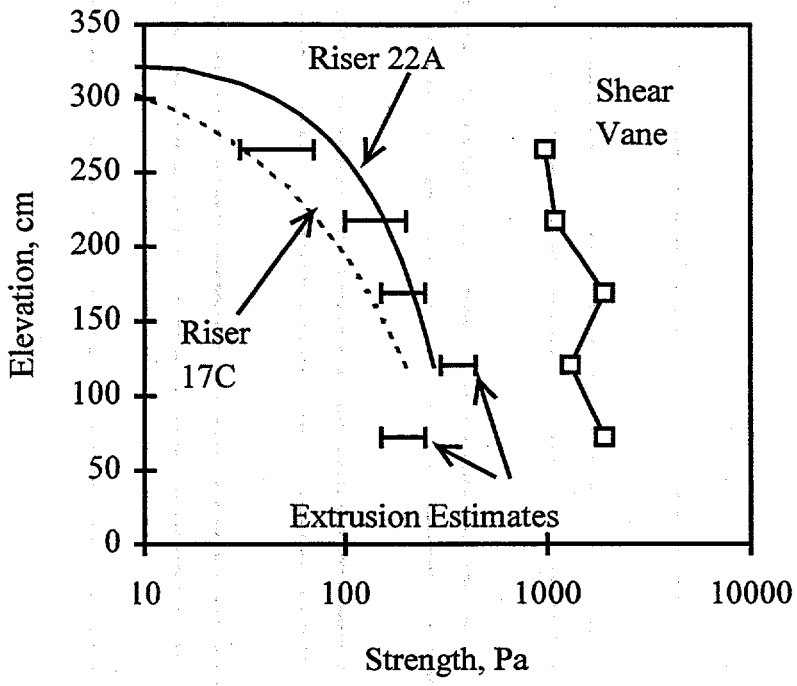

Figure 5.1. Strength Estimates for SY-103

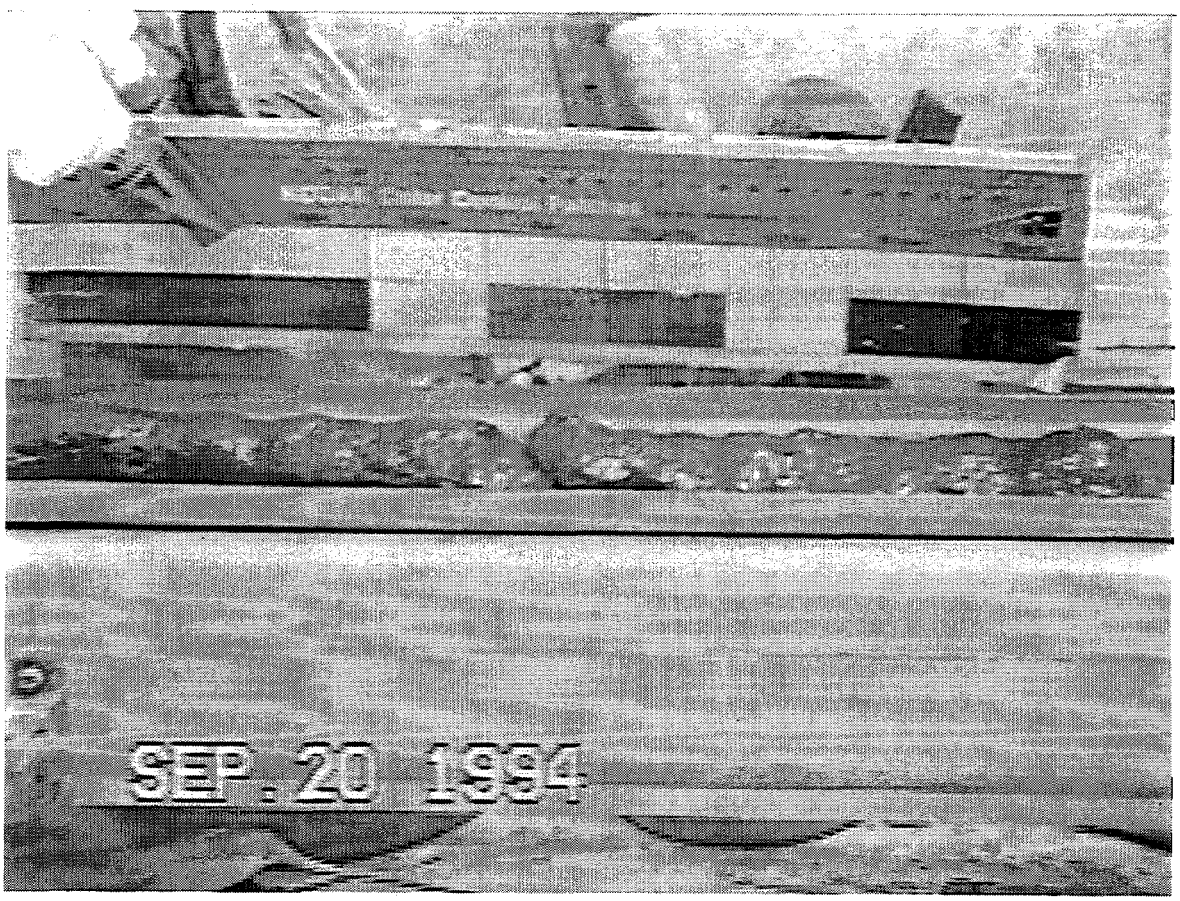

Figure 5.2. Extrusion Behavior for SY-103, Core 62, Segment 10 (estimated shear strength of 30–70 Pa)

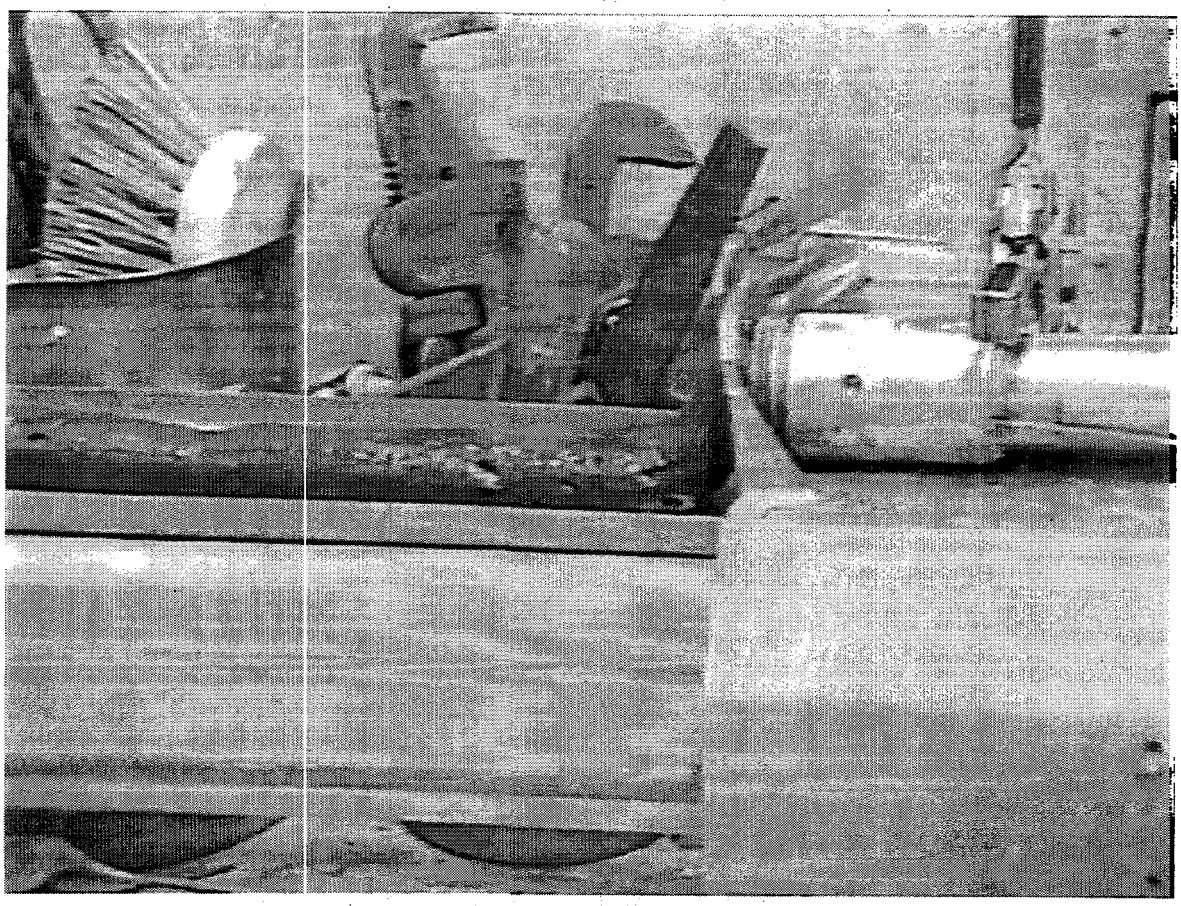

Figure 5.3. Extrusion Behavior for SY-103, Core 62, Segment 11 (estimated shear strength of 100-200 Pa).

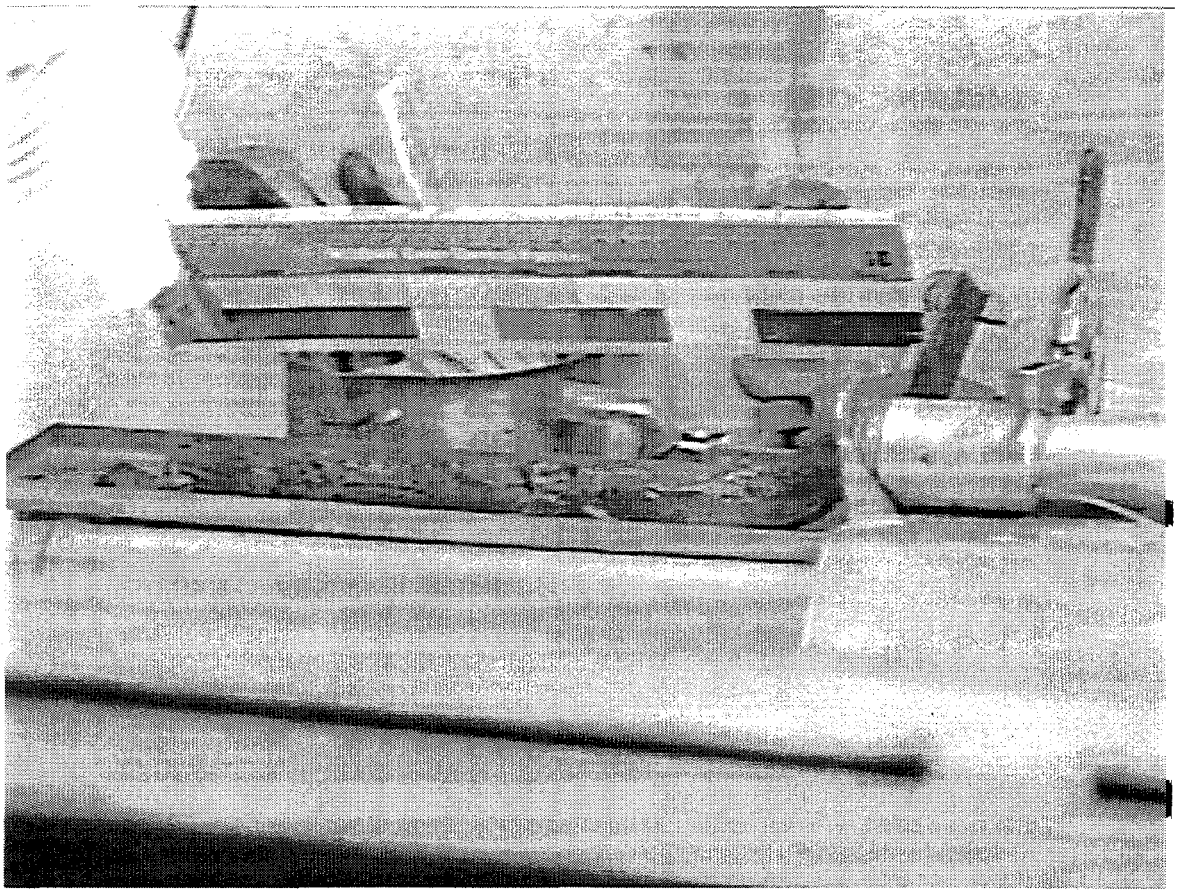

Figure 5.4. Extrusion Behavior for SY-103, Core 62, Segment 12 (estimated shear strength of 150–250 Pa)

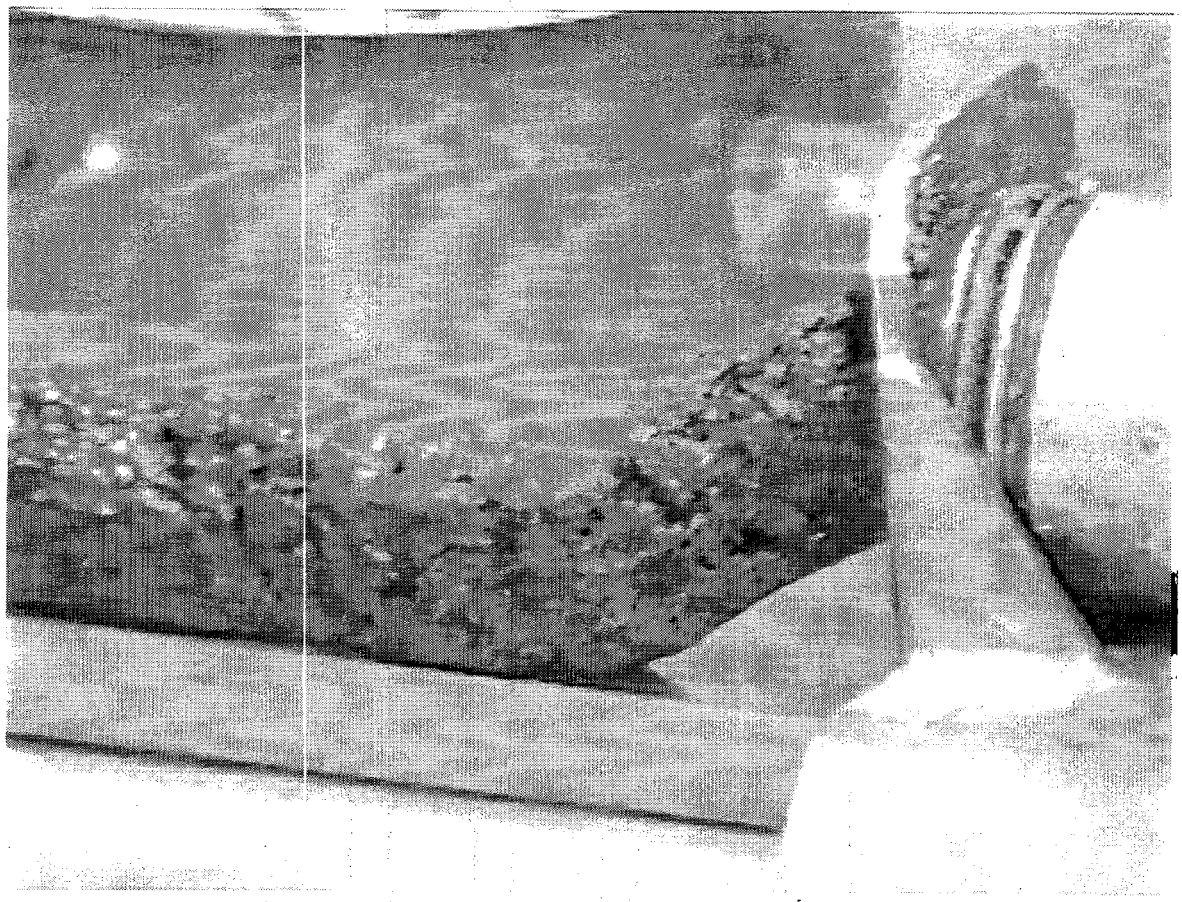

Figure 5.5. Extrusion Behavior for SY-103, Core 62, Segment 13 (estimated shear strength of 300–450 Pa)

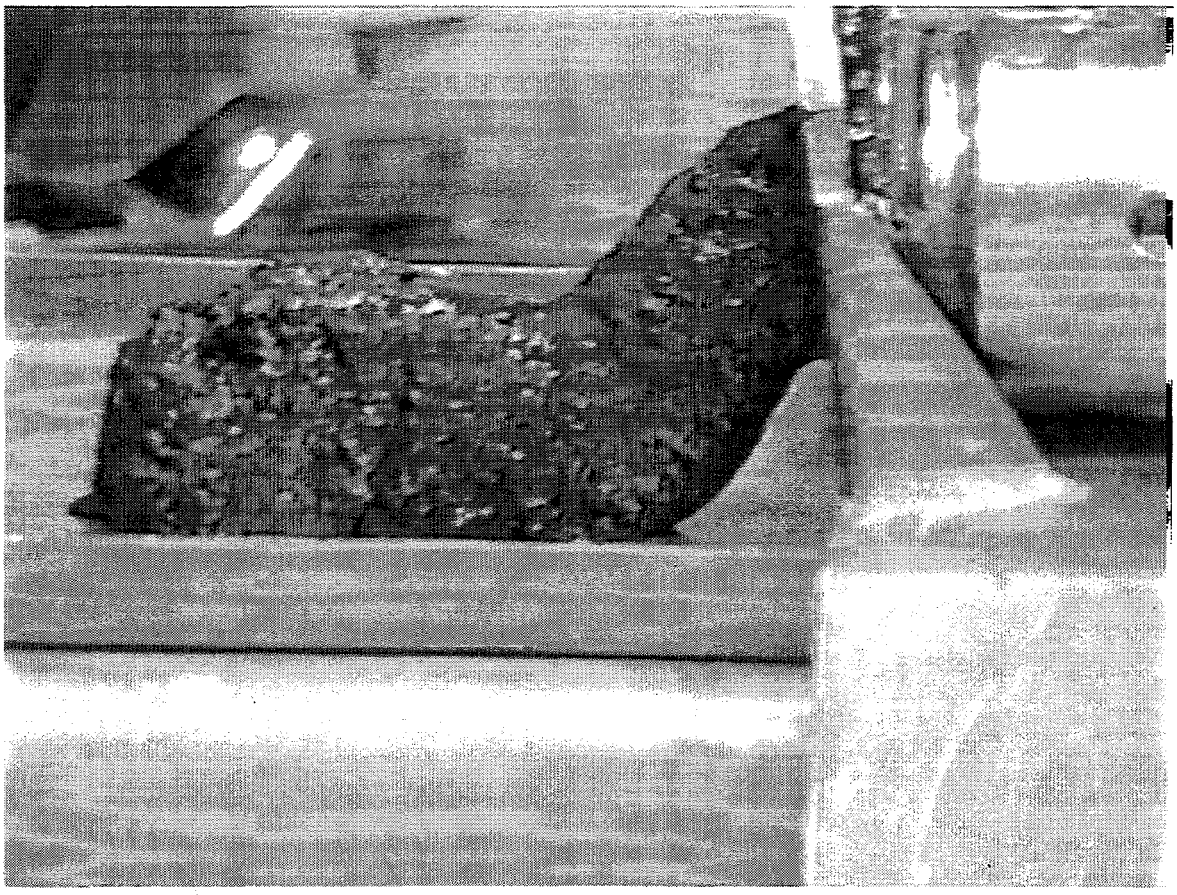

Figure 5.6. Extrusion Behavior for SY-103, Core 62, Segment 14 (estimated shear strength of 150–250 Pa)

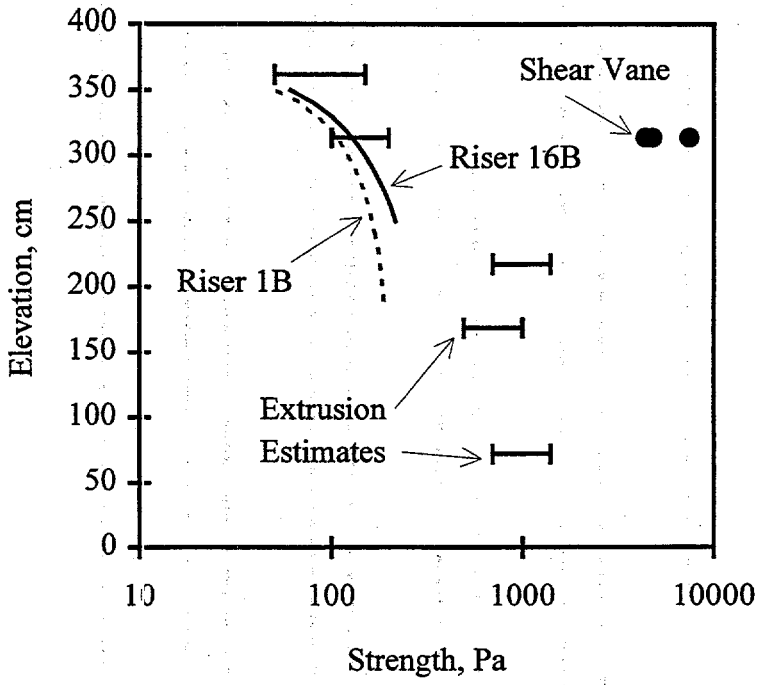

Figure 5.7. Strength Estimates for AN-103

Figure 5.8. Extrusion Behavior for AN-103, Core 167, Segment 11 (estimated shear strength of 50–150 Pa)

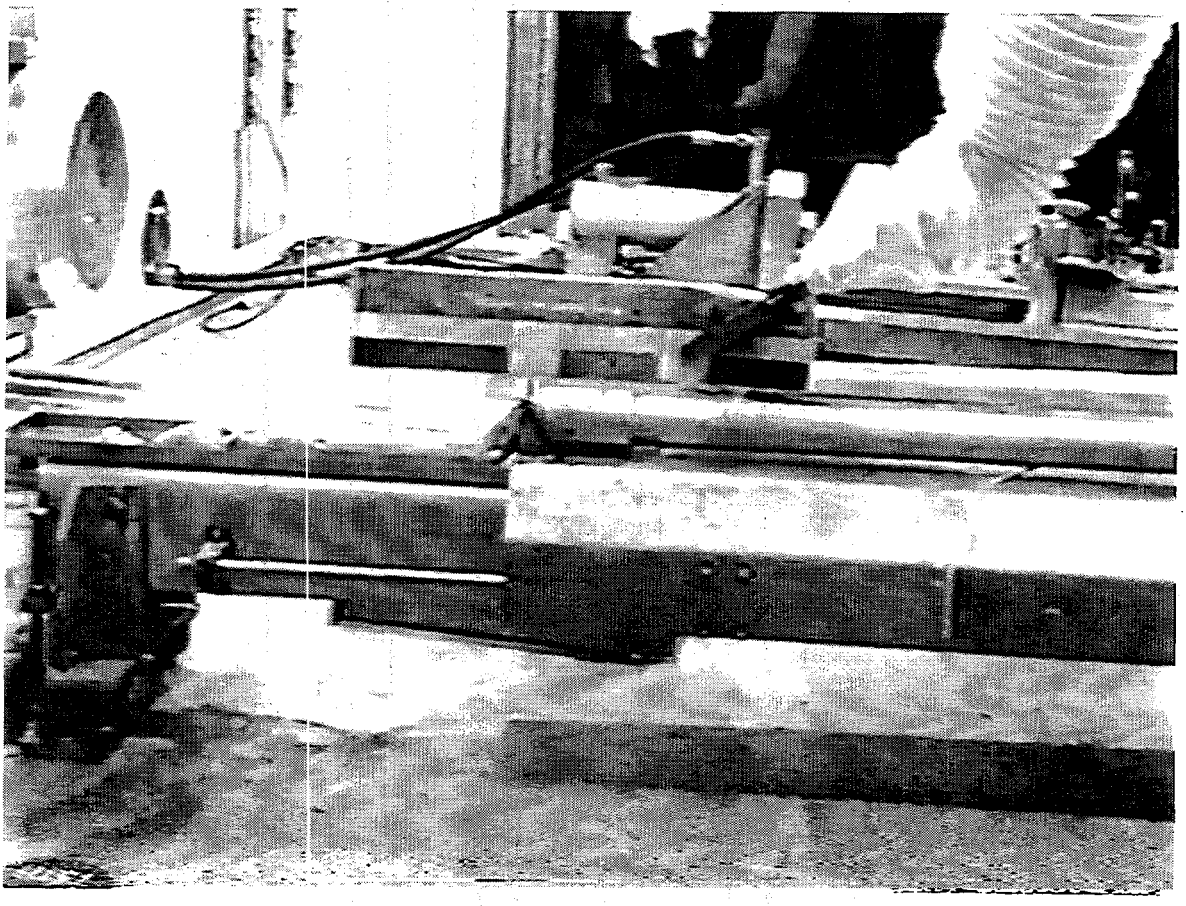

Figure 5.9. Extrusion Behavior for AN-103, Core 167, Segment 12 (estimated shear strength of 100–200 Pa)

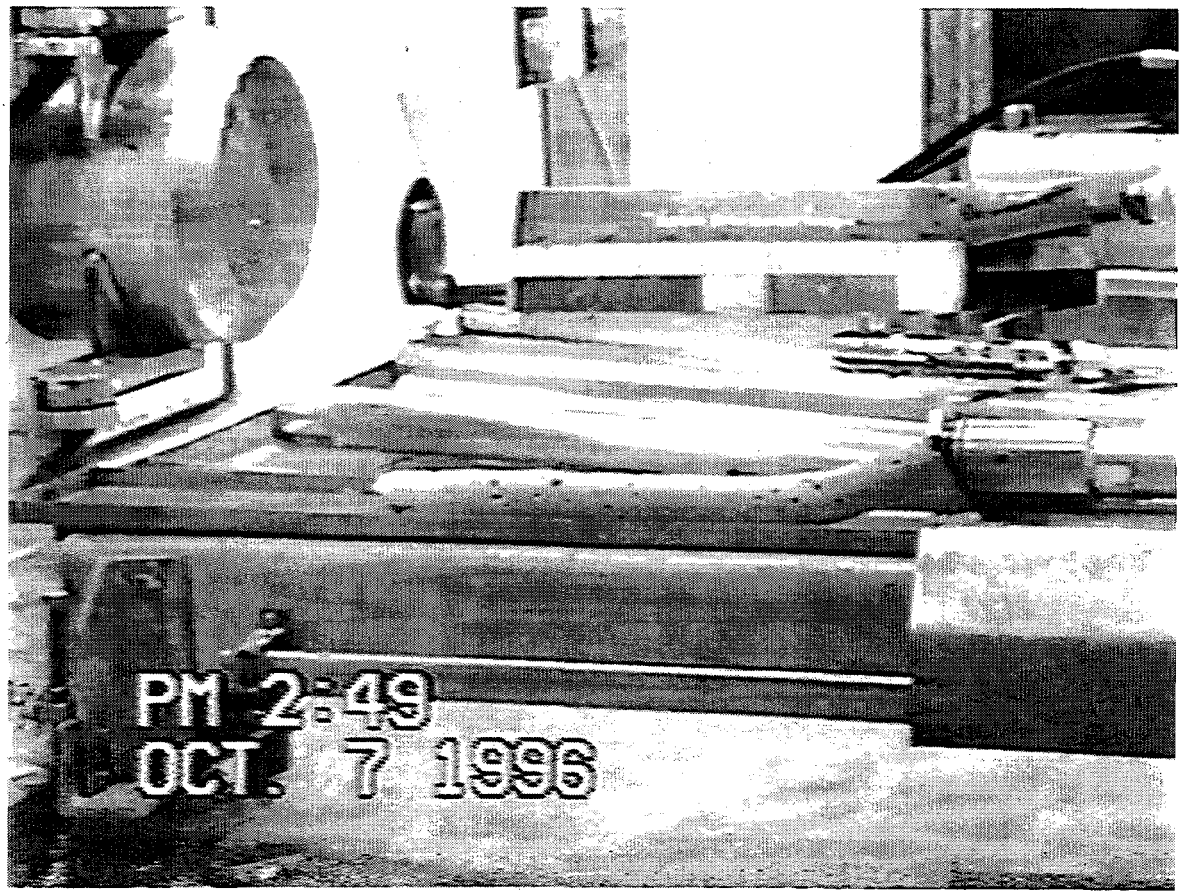

Figure 5.10. Extrusion Behavior for AN-103, Core 167, Segment 14 (estimated shear strength of 700–1400 Pa)

Figure 5.11. Extrusion Behavior for AN-103, Core 167, Segment 15 (estimated shear strength of 500–1000 Pa)

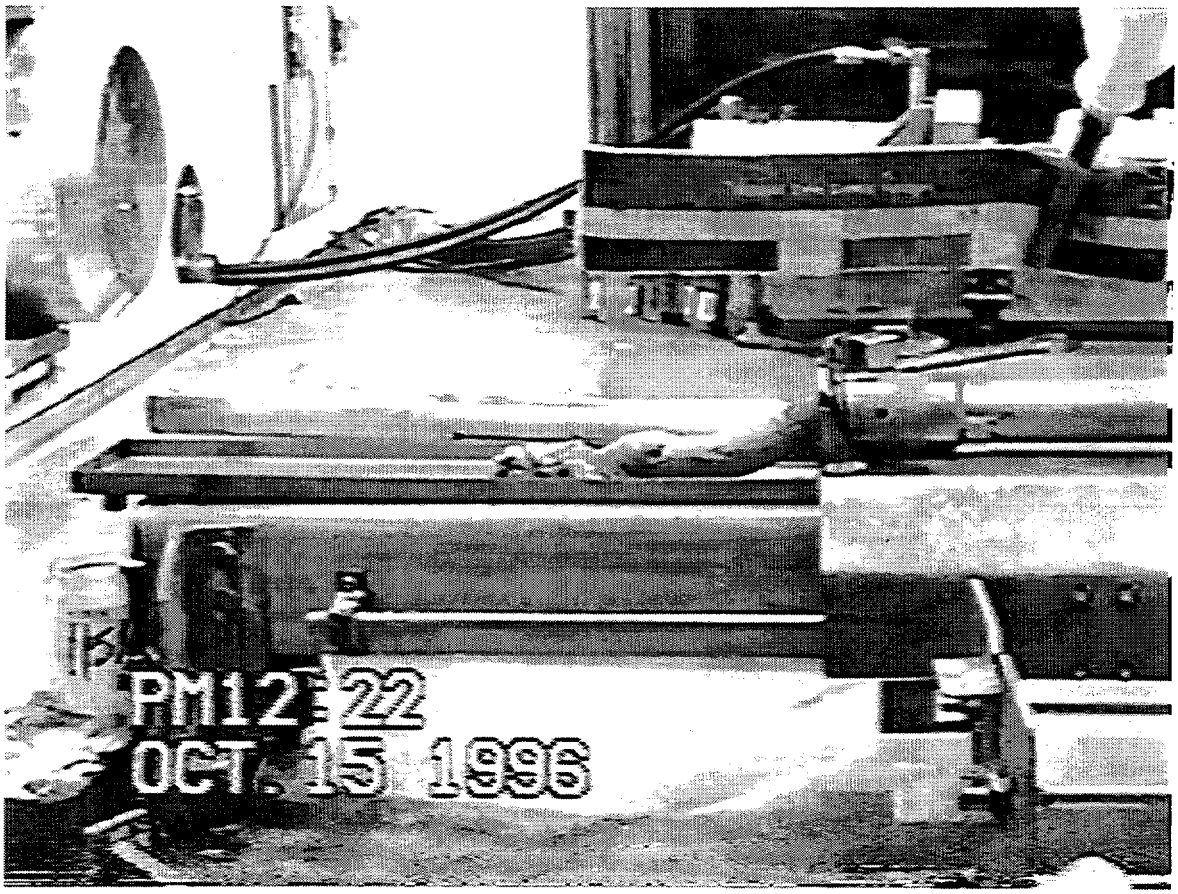

Figure 5.12. Extrusion Behavior for AN-103, Core 167, Segment 17 (estimated shear strength of 700–1400 Pa)

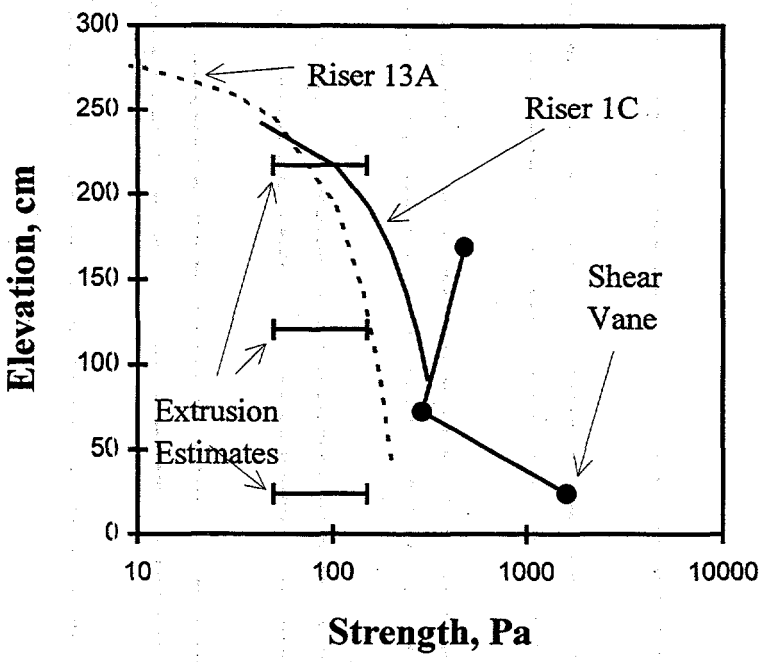

Figure 5.13. Strength Estimates for AW-101

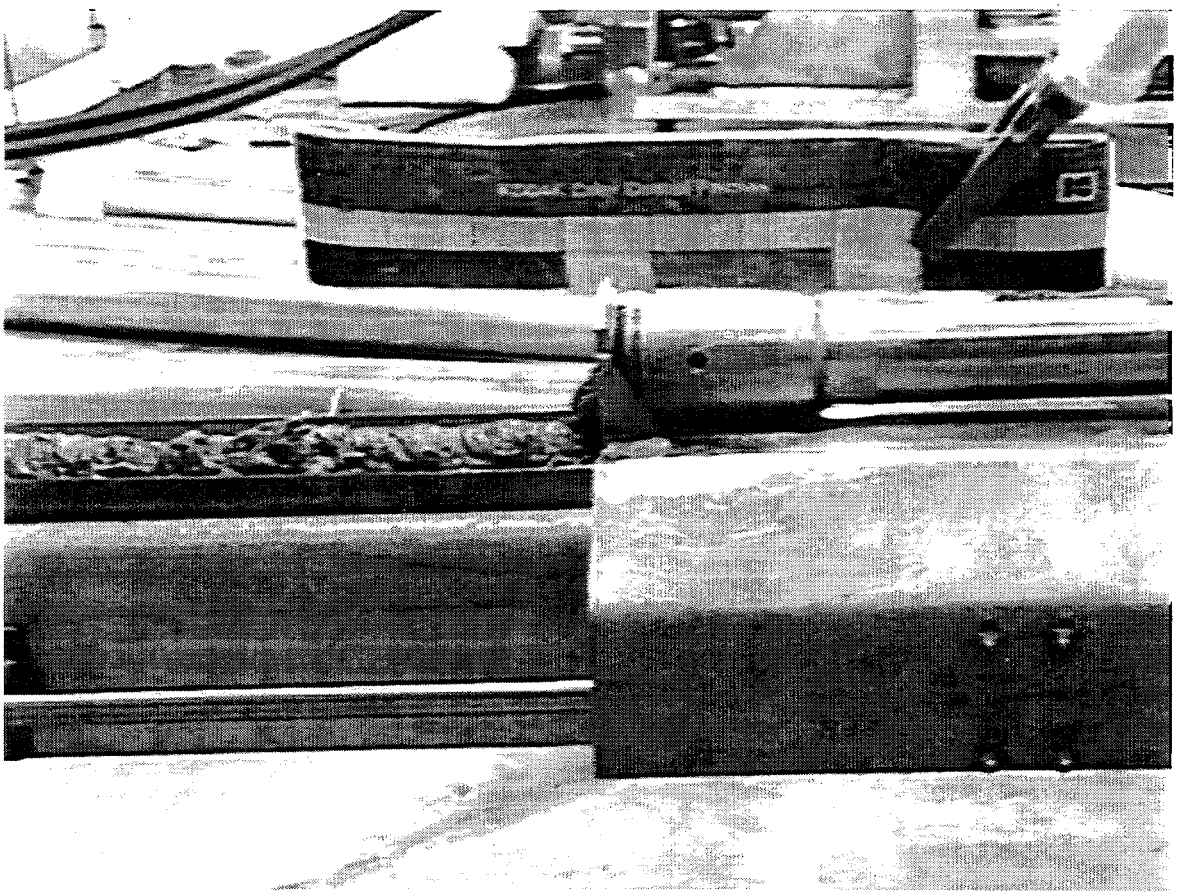

Figure 5.14. Extrusion Behavior for AW-101, Core 132, Segment 18 (estimated shear strength of 50–150 Pa)

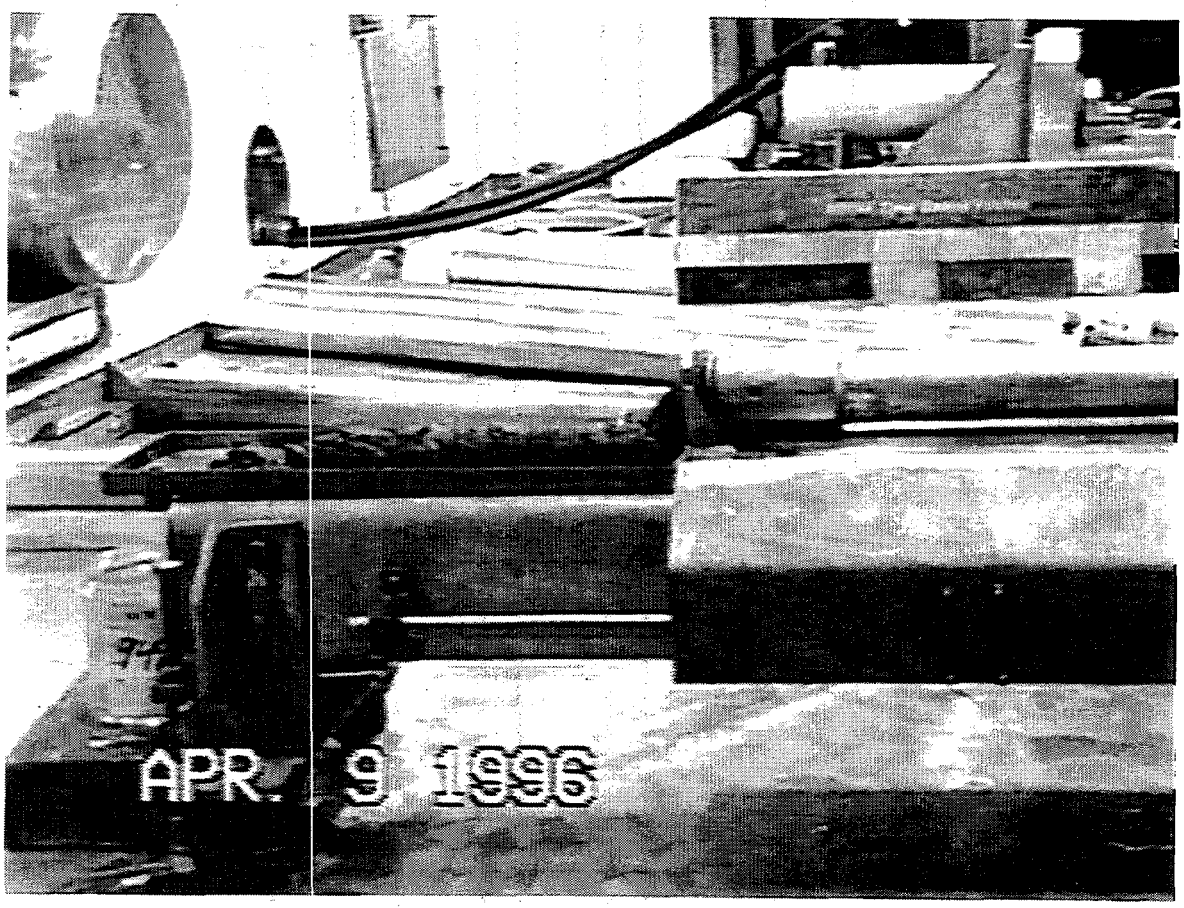

Figure 5.15. Extrusion Behavior for AW-101, Core 132, Segment 20 (estimated shear strength of 50–150 Pa)

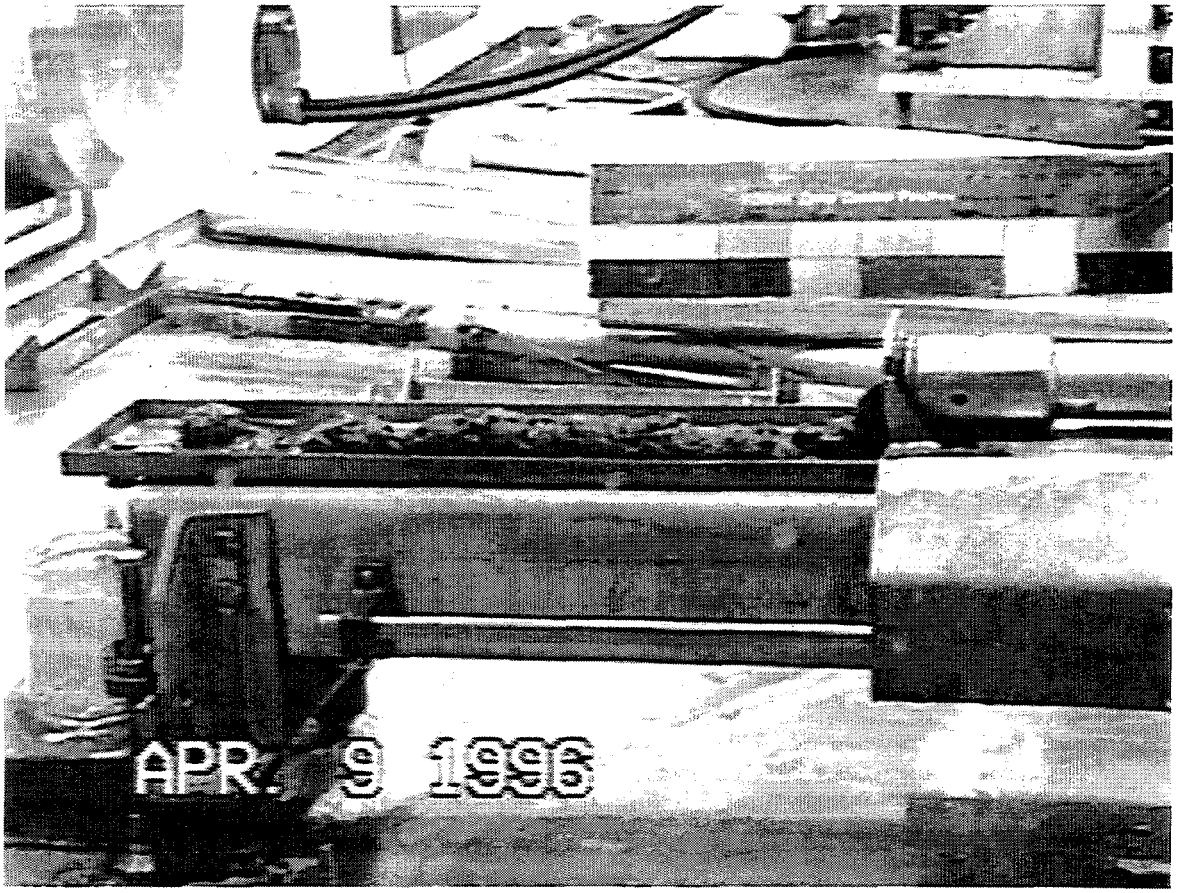

Figure 5.16. Extrusion Behavior for AW-101, Core 132, Segment 22 (estimated shear strength of 50–150 Pa)

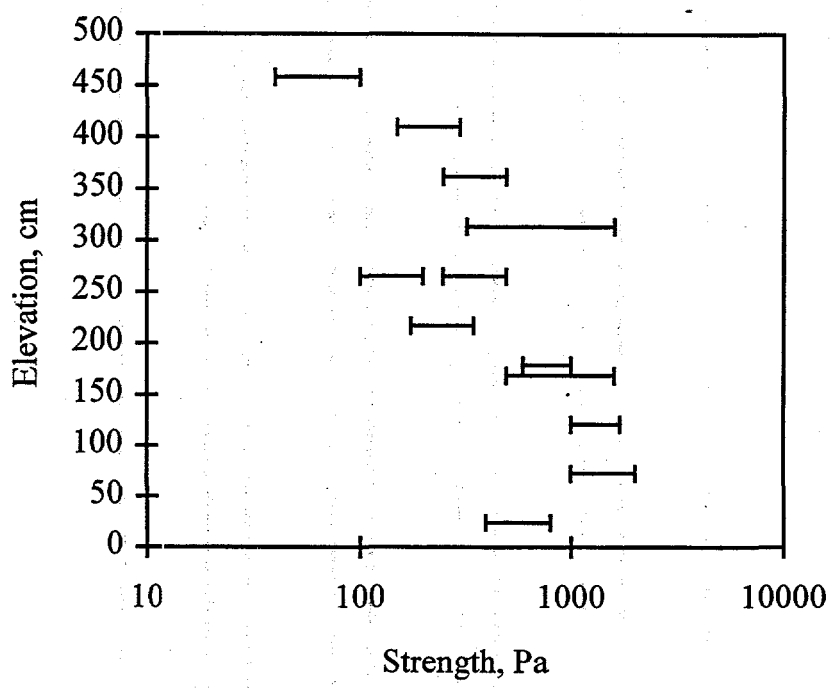

Figure 5.17. Strength Estimates for S-102

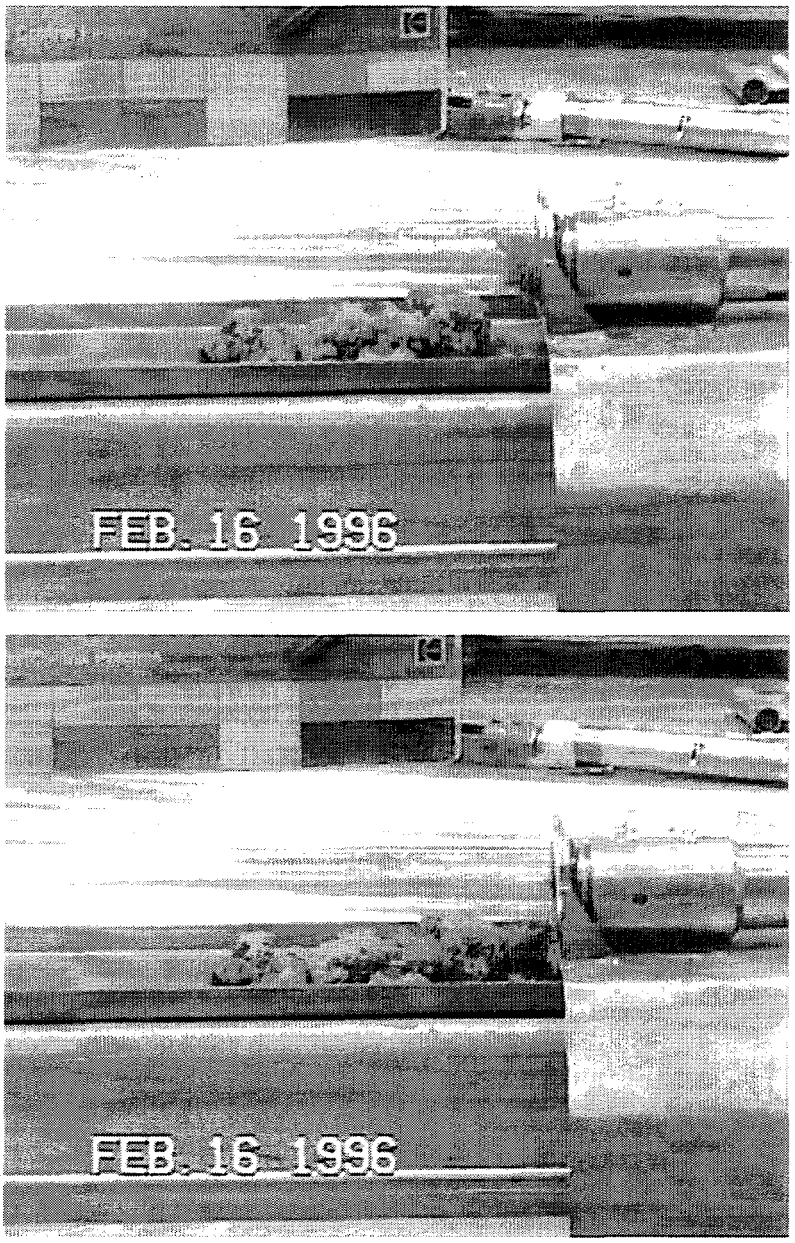

Figure 5.18. Extrusion Behavior for S-102, Core 130, Segment 2 (estimated shear strength of 40–100 Pa)

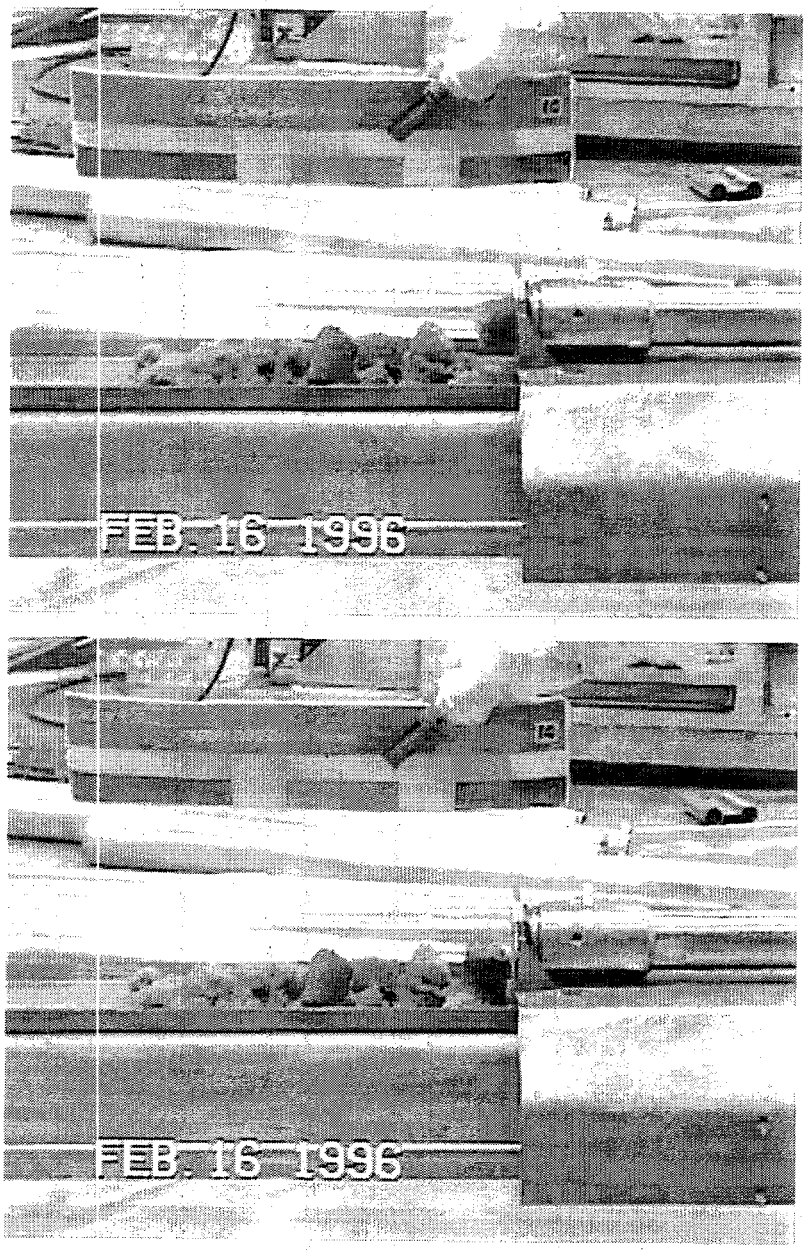

Figure 5.19. Extrusion Behavior for S-102, Core 130, Segment 3 (estimated shear strength of 150–300 Pa)

Figure 5.20. Extrusion Behavior for S-102, Core 130, Segment 4 (estimated shear strength of 250–500 Pa)

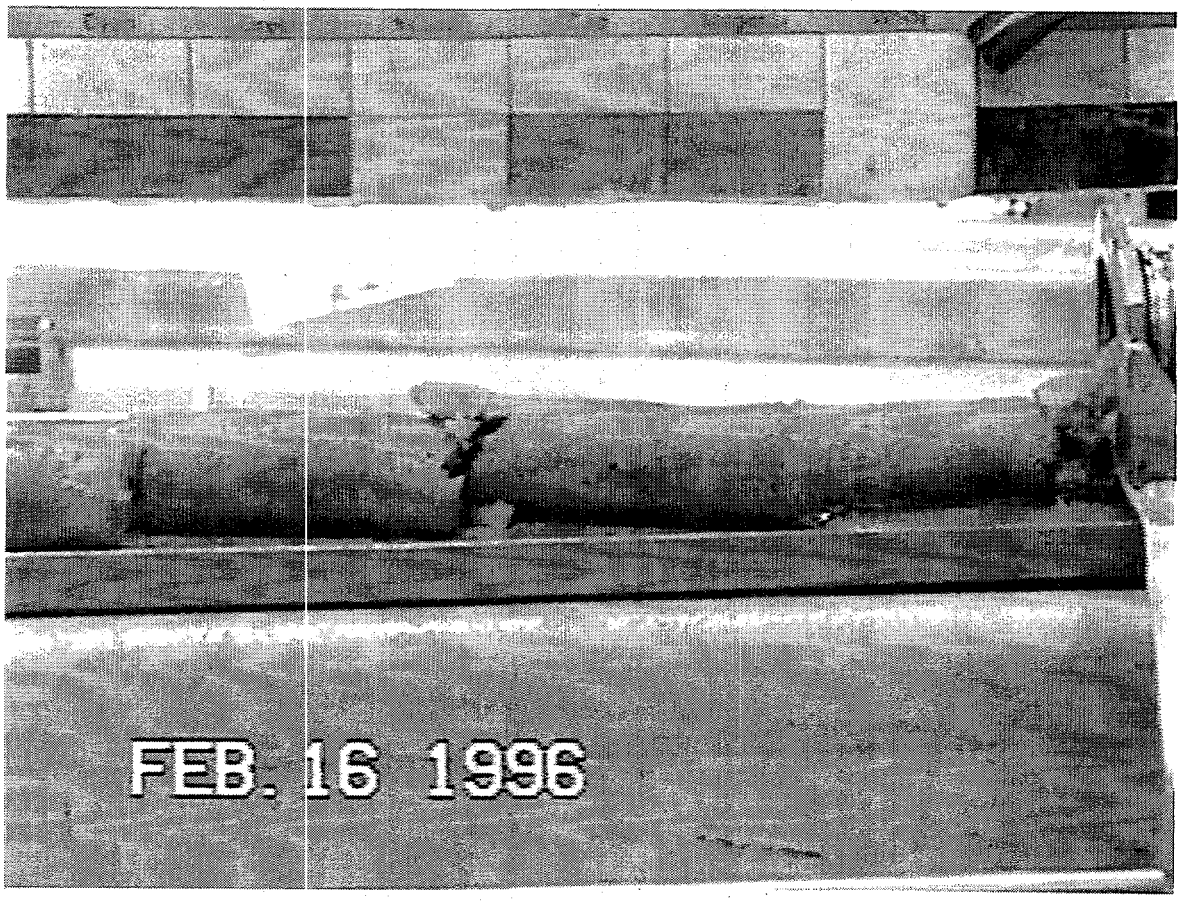

Figure 5.21. Extrusion Behavior for S-102, Core 130, Segment 5 (estimated shear strength of 300–1,600 Pa)

Figure 5.22. Extrusion Behavior for S-102, Core 130, Segment 6a (estimated shear strength of 100–200 Pa)

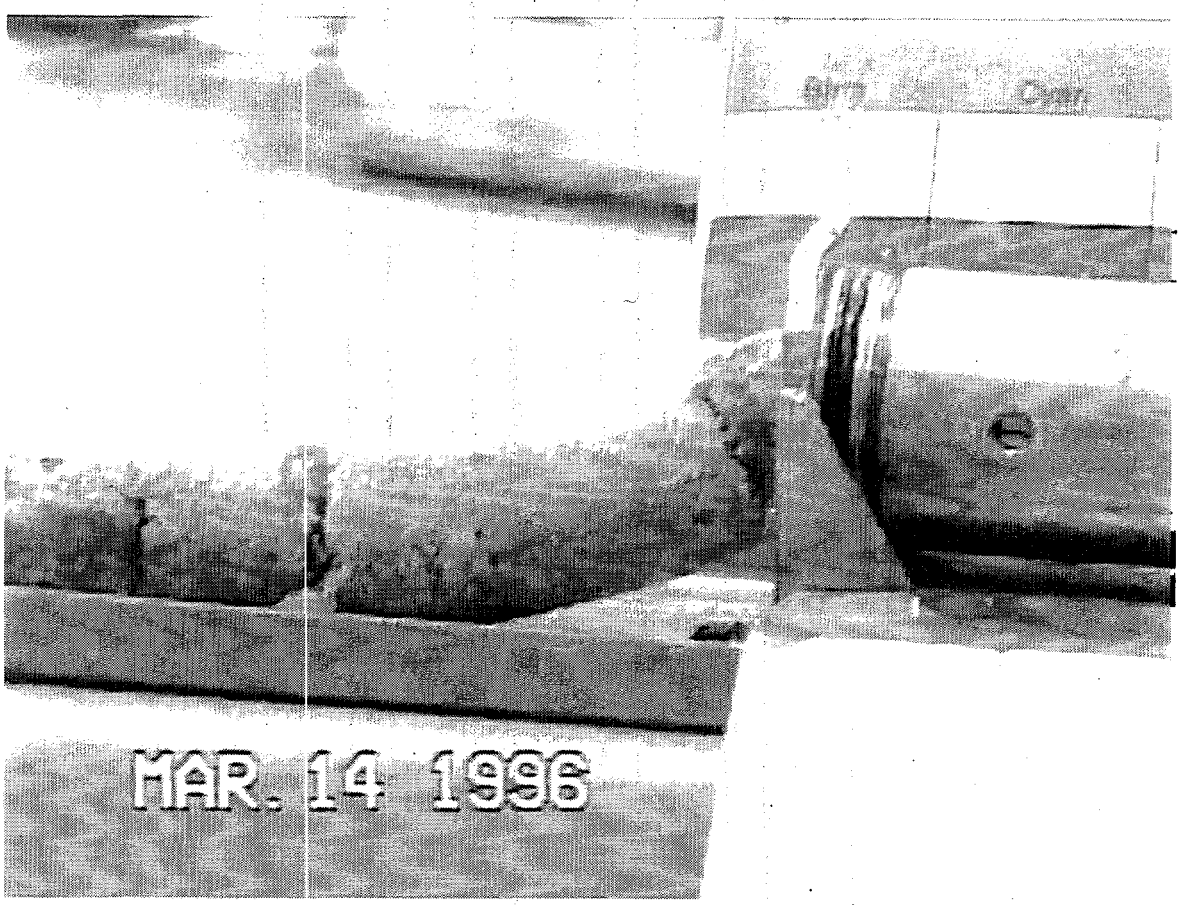

Figure 5.23. Extrusion Behavior for S-102, Core 130, Segment 6b (estimated shear strength of 250–500 Pa)

Figure 5.24. Extrusion Behavior for S-102, Core 130, Segment 7 (estimated shear strength of 175–350 Pa)

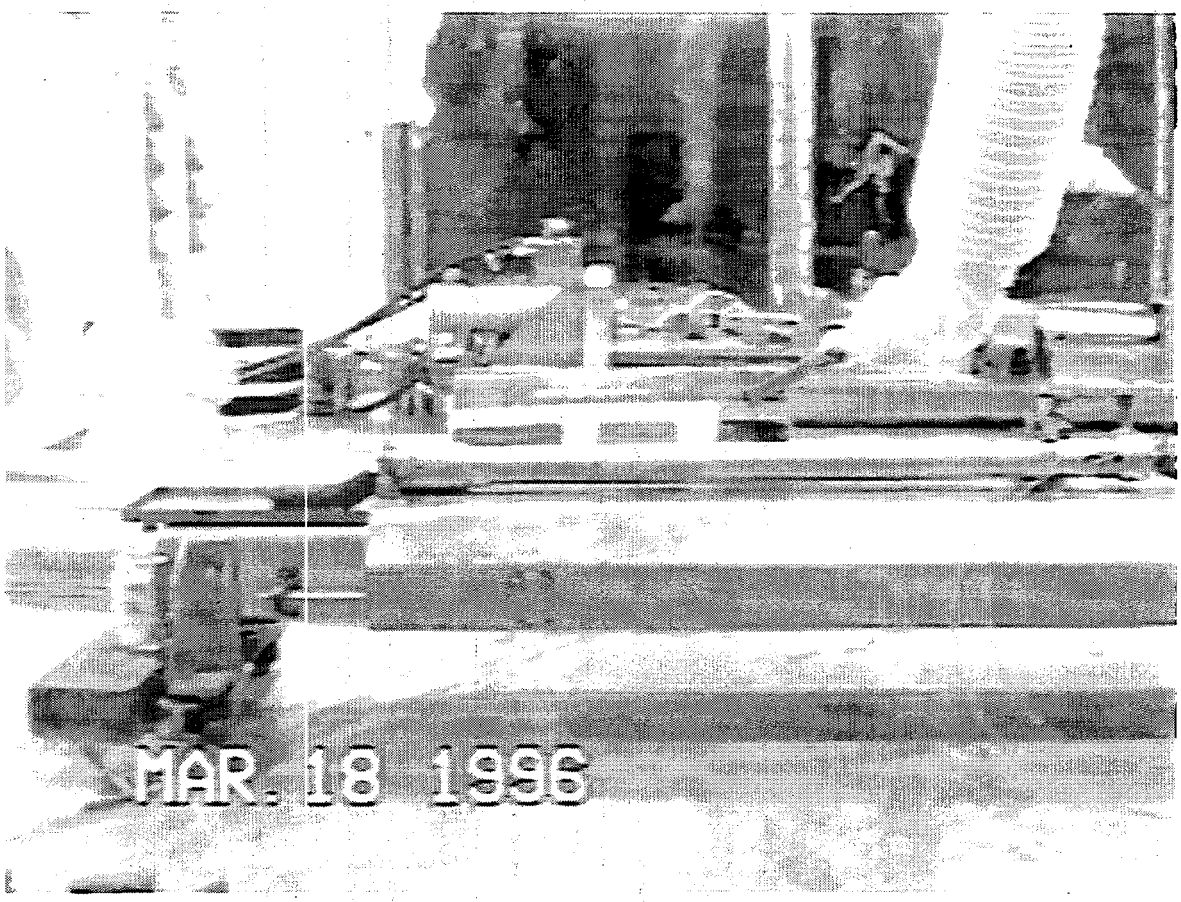

Figure 5.25. Extrusion Behavior for S-102, Core 130, Segment 8a (estimated shear strength of 600–1,000 Pa)

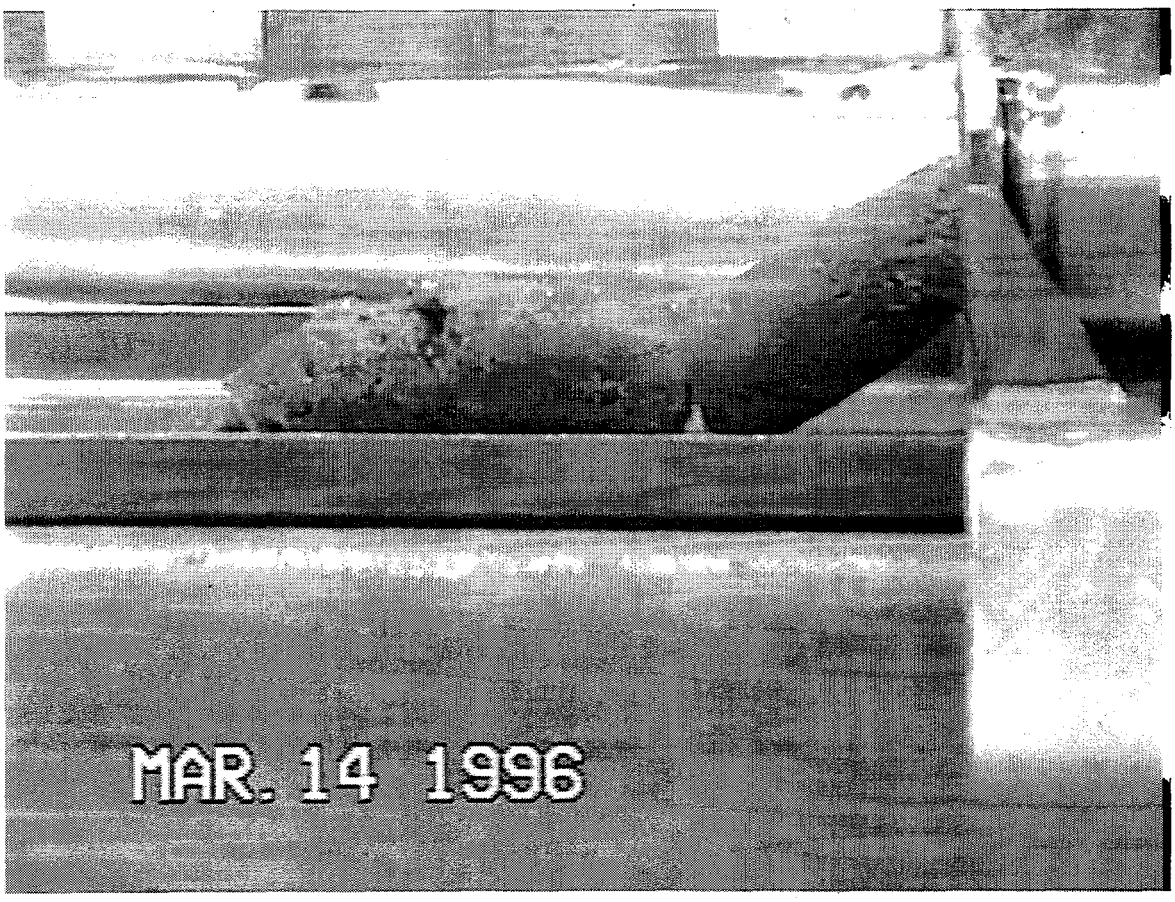

Figure 5.26. Extrusion Behavior for S-102, Core 130, Segment 8b (estimated shear strength of 500–1,600 Pa)

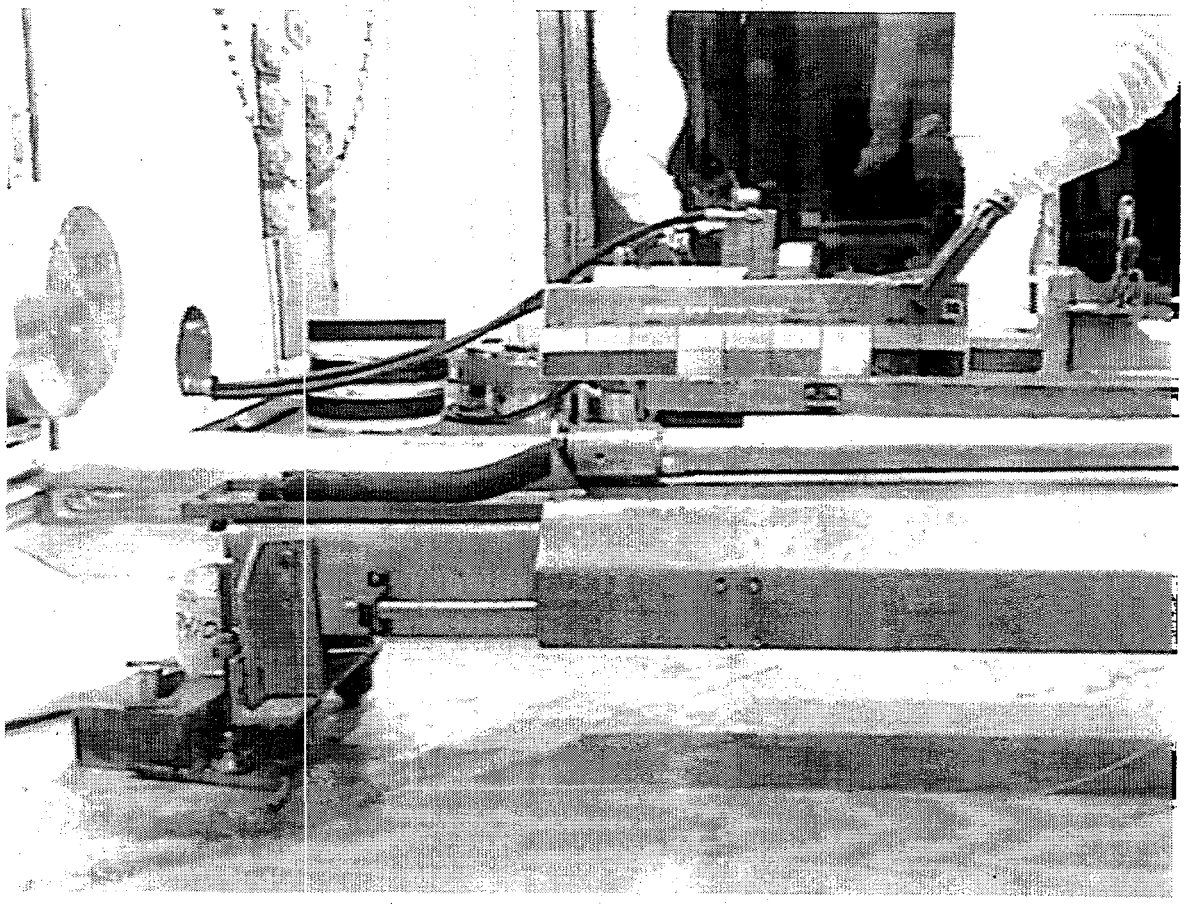

Figure 5.27. Extrusion Behavior for S-102, Core 130, Segment 9 (estimated shear strength of 1,000–1,700 Pa)

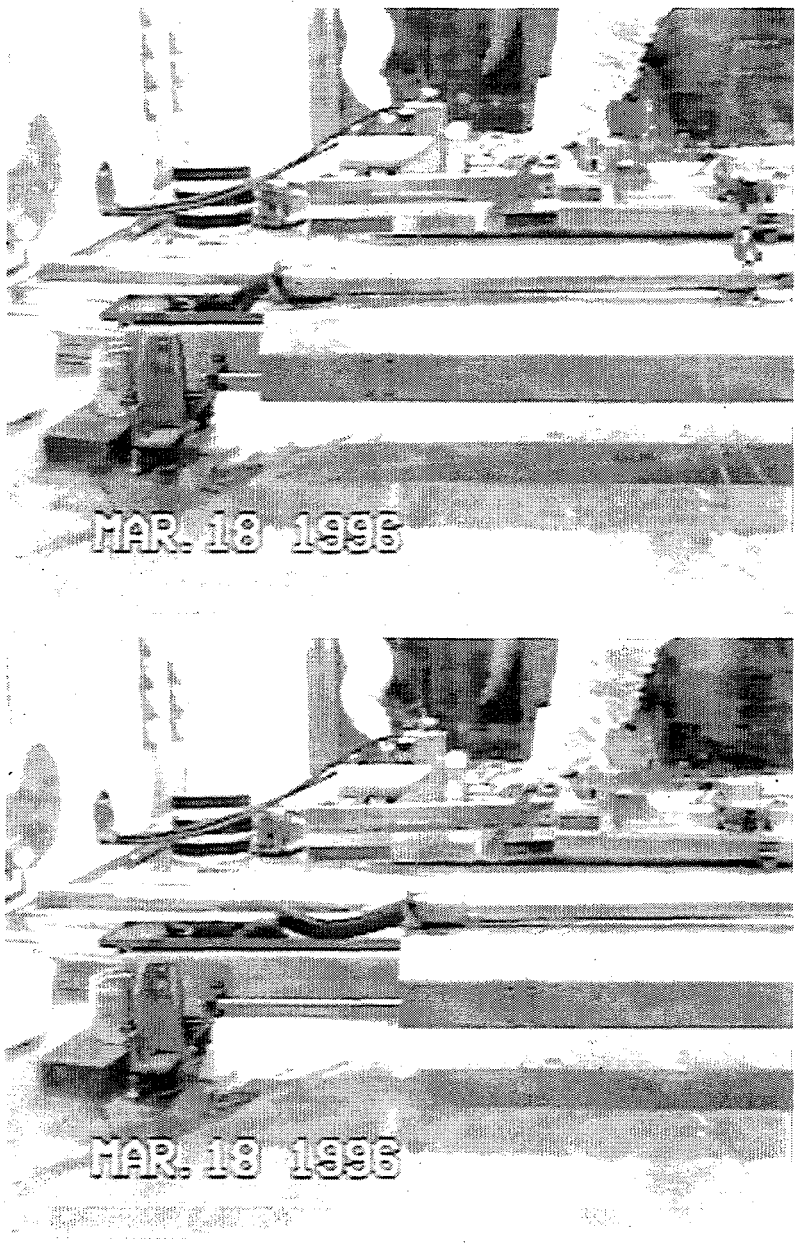

Figure 5.28. Extrusion Behavior for S-102, Core 130, Segment 10 (estimated shear strength of 1,000–2,000 Pa)

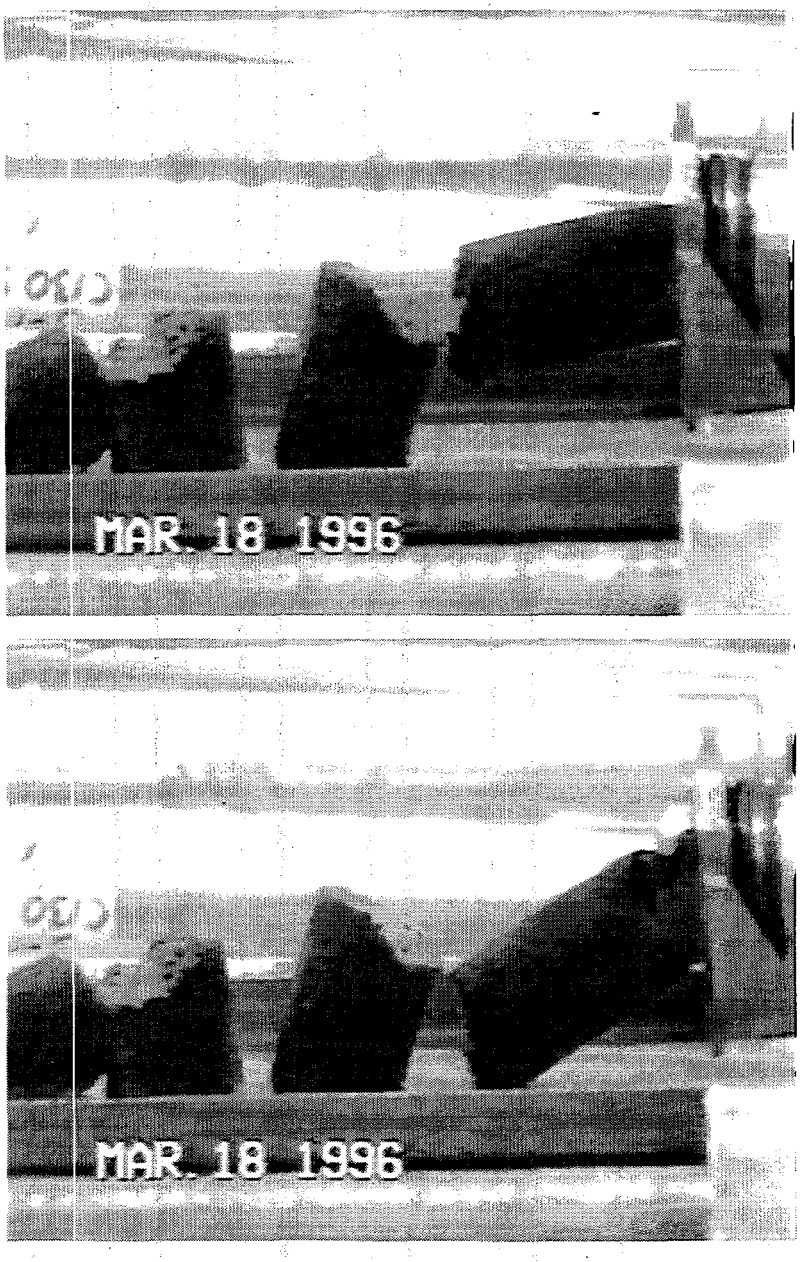

Figure 5.29. Extrusion Behavior for S-102, Core 130, Segment 11 (estimated shear strength of 400–800 Pa)

6.0 Conclusions

A method was developed to obtain strength estimates for actual wastes from observations of the wastes behavior during extrusion from core samplers. These estimates are important because waste strength plays a central role in both the mechanisms of bubble retention and bubble release. The main conclusions of this study are given below.

Results showed a reproducible extrusion behavior for bentonite clay and kaolin/Ludox simulants over strengths ranging from 30 to 6,500 Pa. Video recordings and still images were used to document the extrusion behavior.

The extrusion behavior changed distinctively with variations in strength, forming the basis for creating visual standards.

Strength estimates were made for wastes from DSTs 241-SY-103, 241-AW-101, and 241-AN-103, and SST 241-S-102.

The strength estimates were compared with available in-tank ball rheometer data and laboratory shear vane data. The estimates from horizontal extrusion generally agreed within a factor of 2 with the ball rheometer data, which is acceptable accuracy for use in bubble retention models.

While this initial investigation has been successful in making strength estimates, the simulants investigated did not mimic all of the actual waste behavior, making the strength estimates more uncertain. Accordingly, further simulant studies to develop better visual standards would be useful. In addition, a theory that relates the observed drooping of the actual wastes to strength would substantially strengthen the basis of these estimates.

7.0 References

Gauglitz PA, SD Rassat, PR Bredt, JH Konynenbelt, SM Tingey, and DP Mendoza. 1996. *Mechanisms of Gas Bubble Retention and Release: Results for Hanford Waste Tanks 241-S-102 and 241-SY-103 and Single-Shell Tank Simulants.* PNNL-11298, Pacific Northwest National Laboratory, Richland, Washington.

Gauglitz PA, SD Rassat, MR Powell, RR Shah, and LA Mahoney. 1995. *Gas Bubble Retention and Its Effect on Waste Properties: Retention Mechanisms, Viscosity, and Tensile and Shear Strength.* PNL-10740, Pacific Northwest Laboratory, Richland, Washington.

Hanlon BM. 1995. *Waste Tank Summary Report for Month Ending August 31, 1995.* WHC-EP-0182-89, Westinghouse Hanford Company, Richland, Washington.

Heath WO. 1987. *Development of an In-Situ Method to Define the Rheological Properties of Slurries and Sludges Stored in Underground Tanks.* PNL-6083, Pacific Northwest Laboratory, Richland, Washington.

Johnson GD, WB Barton, JW Brothers, SA Bryan, PA Gauglitz, RC Hill, LR Pederson, CW Stewart, and LM Stock. 1997. *Flammable Gas Project Topical Report.* HNF-SP-1193 Rev. 2 (PNNL-11500), Lockheed Martin Services Hanford, Richland, Washington.

Meyer PA, ME Brewster, SA Bryan, G Chen, LR Pederson, CW Stewart, and G Terrones. 1997. *Gas Retention and Release Behavior in Hanford Double-Shell Waste Tanks.* PNNL-11536 Rev. 1, Pacific Northwest National Laboratory, Richland, Washington.

Powell MR, CM Gates, CR Hymas, MA Sprecher, and NJ Morter. 1995. *Fiscal Year 1994 1/25-Scale Sludge Mobilization Testing.* PNL-10582, Pacific Northwest Laboratory, Richland, Washington.

Rassat SD, PA Gauglitz, PR Bredt, LA Mahoney, SV Forbes, and SM Tingey. 1997. *Mechanisms of Gas Bubble Retention and Release: Experimental Results for Hanford Waste Tanks 241-A-101 and 241-AN-103.* PNNL-11642, Pacific Northwest National Laboratory, Richland, Washington.

Stewart CW, JM Alzheimer, ME Brewster, RE Mendoza, HC Reid, CL Shepard, and G Terrones. 1996a. *In Situ Rheology and Gas Volume in Hanford Double-Shell Waste Tanks.* PNNL-11296, Pacific Northwest National Laboratory, Richland, Washington.

Stewart CW, ME Brewster, PA Gauglitz, LA Mahoney, PA Meyer, KP Recknagle, and HC Reid. 1996b. *Gas Retention and Release Behavior in Hanford Single-Shell Waste Tanks.* PNNL-11391, Pacific Northwest National Laboratory, Richland, Washington.

Distribution

No. of Copies

Offsite

2 Office of Scientific and Technical Information

2 Los Alamos National Laboratory
P.O. Box 1663
Los Alamos, NM 87545
Attn: D. R. Bennett, K575
J. R. White, K575

S. E. Slezak
Sandia National Laboratory
P.O. Box 5800 MS 1004
Albuquerque, NM 87110

B. C. Hudson
P.O. Box 271
Lindsborg, KA 67456

J. L. Kovach
Nuclear Consulting Services, Inc.
P.O. Box 29151
Columbus OH, 43229-0151

T. E. Larson
CR SubTAP
2711 Walnut St.
Los Alamos NM, 87544

No. of Copies

Onsite

2 DOE Richland Operations Office

C. A. Groendyke	S7-54
G. W. Rosenwald	S7-54

11 Project Hanford Management Contract Team

R. Akita	T6-20
W. B. Barton	R2-11
R. E. Bauer	S7-14
B. Griffin II	T6-30
K. M. Hodgson	R2-11
G. D. Johnson (3)	S7-15
N. W. Kirch	R2-11
J. W. Lentsch	S7-15
D. A. Reynolds	R2-11

22 Pacific Northwest National Laboratory

S. Q. Bennett	K7-90
P. R. Bredt	P7-25
J. W. Brothers (3)	K9-20
P. A. Gauglitz (5)	P7-41
L. M. Peurrung	P7-41
M. R. Powell (3)	P7-41
S. D. Rassat	P7-41
A. Shekarriz	K7-15
C. W. Stewart	K7-15
Information Release (5)	K1-06